# Diffractive production of $S$ and $D$ wave vector mesons in Deep Inelastic Scattering

Igor Ivanov

Novosibirsk University, Russia

and

Forschungszentrum Juelich, Germany

Scientific advisors:

**Prof.Univ. Dr. J.Speth** (KFA, Jülich)
**Prof. N.N.Nikolaev** (KFA, Jülich and ITP, Moscow)
**Prof. I.F.Ginzburg** (IM, Novosibirsk)

Jülich — 1999

# Abstract

In this work the production of vector mesons in diffractive DIS is analyzed, with an emphasis on the impact of the internal spin structure of a vector meson upon its virtual photo-production rate. For the first time, the full sets of $s$-channel helicity conserving and violating amplitudes were derived for pure $S$ and $D$ wave vector mesons. In the course of analytical and numerical investigation, we found a striking difference between $S$ and $D$ wave vector meson production. First, in the case of helicity conserving amplitudes, $D$ wave vector mesons were found to exhibit dramatically different $Q^2$-behavior due to abnormally large higher twist contributions. Besides, we found that helicity conserving amplitudes for $S$ and $D$ states are numerically comparable, which makes the physical $\rho$ meson very sensitive to $D$ wave admixture. Second, the helicity violating amplitudes in light vector meson production turned out large both for $S$ and $D$ wave states. In the case of heavy quarkonia, these amplitudes became suppressed by the non-relativistic motion for $S$ wave mesons but they were still large for $D$ wave states.

Aiming at producing sort of a manual on the diffractive vector meson production, we carried out all calculations in a pedagogical manner with maximally full presentation of intermediate steps and accompanied them with detailed qualitative discussion.

# Contents

# 1    Introduction

In the past 30 years the particle physics theory has proved numerous times to provide a good, consistent, unified description of the great variety of nuclear, low and high energy particle physics experiments. Being based on the ideas of QFT applicability, gauge approach to fundamental interactions, symmetry and naturalness considerations, the Standard Model managed to explain virtually all phenomena in electromagnetic, weak and strong interactions, to predict new particles and effects. Though the questions of fundamental origin lie beyond the scope of the Standard Model, its precision in description, for instance, QED phenomena reaches the magnitude of $10^{-10}$.

However, the current situation is not that optimistic in the domain of strong interactions. The gauge–based formulation — the Quantum Chromodynamics (QCD) — seems to offer reasonably good description only of the energetic enough processes (more accurately: only when every vertex involves at least one highly virtual particle) thanks to the famous asymptotic freedom. The major difficulty lies in the behavior of the QCD coupling constant: $\alpha_s(Q^2)$ exhibits infrared growth and becomes comparable to unity at $Q^2 \sim 1$ GeV$^2$. The net result is that the perturbation theory — the only prolific universal treatment of various high-energy processes — fails to give even qualitative description of low-energy, essentially non-perturbative phenomena. Additional difficulties arise from the non-abelian nature of QCD, chiral symmetry breaking, non-trivial QCD vacuum, instantons etc.

On the other hand, many separate concepts have been developed, which do not cling to the perturbative QCD (pQCD) and provide reasonably good description of phenomena in their applicability regions. The fundamental problem of the theory of strong interactions is that these heterogeneous approaches do not match[1]. They do not comprise a unified picture of strong interactions. Given such a lack of universal, rigorously derived results, one must admit that the subject of our investigation belongs to the realm of phenomenology rather than rigorous theory.

## 1.1    Diffractive processes and Pomeron

In the light of these problems, the careful examination of regions where two or more approaches overlap (or visa versa, where neither of the concepts exhausts the interaction) are of great interest. Diffractive Deep Inelastic Scattering (DIS) is exactly one of these fields.

A typical hard DIS process (Fig.1a) occurs when a virtual photon[2] strikes a proton to produce a hard system $X$ with large invariant mass[3] $s$ and large enough multiplicity, final state hadrons being distributed over whole rapidity range approximately smoothly.

However, as it was noted long ago, sometimes the proton survives, being only slightly deflected, and a virtual photon turns into a so-called diffractive system $X_{diffr}$ with invariant mass $M_{diffr}^2 \ll s$. In this process the proton and the diffractive system are naturally separated

---

[1] Just a few examples of poor accordance among various approaches: the quark generated ladder diagrams do not appear to correspond uniquely to any of experimentally observed Regge trajectories. Another example is the vague status of $\alpha_s =$ const BFKL results in true QCD.

[2] We will always imply that the virtual photon is emitted by an electron, which means the photon is always space-like: if $q$ is photon momentum, then $Q^2 \equiv -q^2 > 0$.

[3] In hard DIS phenomenology this quantity is usually labeled as $W^2$. However, for simplicity we will use notation $s$.
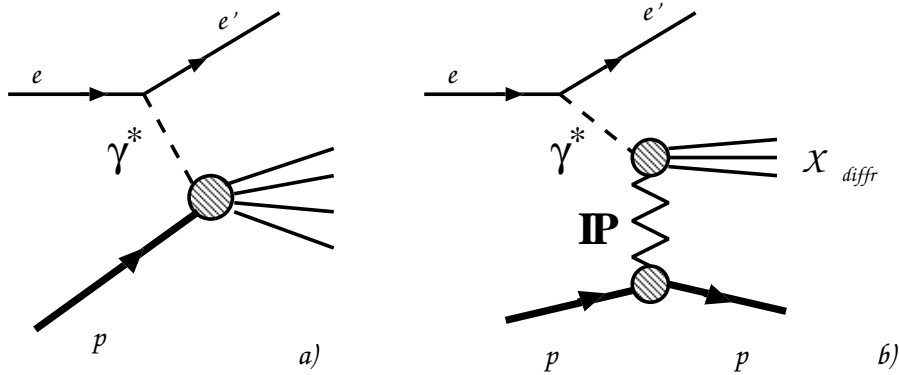
Figure 1: Examples of deep inelastic scattering process: *(a)* hard DIS and *(b)* diffractive DIS. In the latter case $M^2_{diffr} \ll s$ and the process proceeds via pomeron $t$-channel exchange.

by a large rapidity gap and a condition which appears necessary for the rapidity gap formation is $Q^2 \ll s$, or in terms of Bjorken $x$

$$x = \frac{Q^2}{s} \ll 1 \,. \tag{1}$$

This is one of the most common cases of diffractive DIS (DDIS) processes. In fact, the class of diffractive processes is not confined within DIS; it is much broader. There are many other reactions which possess the generic features — the rapidity gap and smallness of $M^2_{diffr}$ — and therefore can be classified as diffractive processes (for a recent review see [1]).

How can a typical diffractive process occur? Certainly, it must be kind of a peripheral interaction: if the photon struck directly one of the valence quarks, the proton would 'explode', providing no way for the large rapidity gap formation. What remains is the possibility of the $t$–channel exchange by not-too-energetic 'particle' (Fig.1b), which would be a natural mechanism of the experimentally observed weak proton deflection and small $M^2_{diffr}$. Further experimental features suggest that this 'particle' should be chargeless and colorless, its interaction with other particles should be of strong (not EM or weak) nature, its 'propagation' should be independent of the specific process ($\gamma p$, $\gamma\gamma$, $pp$, $p\bar{p}$, etc), and it should be of spin 1 (due to approximately $s$–constant $pp$ cross section). In the early 60s this 'particle' was dubbed **Pomeron** (symbol **IP**).

Further properties come from combining the Regge picture and BFKL results with experimental observations (for a detailed review of Regge theory see [2]). They include, first of all, the asymptotic equality of total $pp$ and $p\bar{p}$ cross sections (the Pomeranchuk theorem). Formulated long ago, it was experimentally verified only recently. Then, the Regge theory predicts the power-like $s$-dependence of the total $pp$ cross section $\sigma \propto s^{2(\alpha_{\mathbf{IP}}-1)}$, which has also been experimentally observed, with intercept $\delta_{\mathbf{IP}} \equiv \alpha_{\mathbf{IP}} - 1 \approx 0.08$. On the other hand, the BFKL equation [3, 4] succeeded in reproducing such power-like dependence in QCD, but in a simplified case $\alpha_s =$const. In this approach the hard pomeron is treated as two reggeized gluons — an ansatz used currently in diffraction phenomenology with great success. However, the predictive power of the BFKL approach for the numerical value of the pomeron intercept is still limited and not all issues with sensitivity of the result to the infrared region have been understood. For further reading on pomerons, a topic very intriguing by itself, we refer to [5].

## 1.2 Vector meson production in diffractive DIS

There are several possible final states $X$ in a typical diffractive DIS (DDIS) process $\gamma^* p \to Xp$: system $X$ can be a real photon, a $q\bar{q}$ continuum pair forming two jets or $q\bar{q}$ bound state, for example, a vector meson. Let us now focus specifically on exclusive vector meson production in diffractive DIS. This reaction has been studied extensively at fixed target DIS experiments at CERN and FNAL and more recently by the H1 and ZEUS collaborations at HERA.

In an off-forward scattering $\gamma^*_{\lambda_\gamma} \to V_{\lambda_V}$ the $s$-channel helicity flip amplitudes can be non-vanishing. Because of the well known quark helicity conservation in high energy QCD scattering, such a helicity flip is possible only due to the internal motion and spin–angular momentum coupling of quarks in a vector meson. This issue was accurately analyzed only in very recent papers [6, 7], where it was shown that helicity non-conserving amplitudes are not negligible, as they had been thought before. Thus, as such, the helicity flip amplitudes would offer a great deal of unique information of internal constituent motion and spin–angular momentum structure of vector mesons, unaccessible in other experiments. In addition, the vector meson decays are self-analyzing and the full set of helicity amplitudes can be measured experimentally. For unpolarized incident leptons, the angular distribution of decay products is parameterized in terms of 15 spin-density matrix elements, which can be calculated via 5 — 2 helicity conserving plus 3 helicity violating — basic helicity amplitudes [8].

Despite the great deal of theoretical work on vector meson production in diffractive DIS [6, 7, 9, 10], the above issue of sensitivity to the spin–angular momentum coupling has not been addressed before. Namely, in a typical vector meson production calculation, a vector meson has been implicitly taken as $1S$ state and at the same time an unjustified ansatz was used for $q\bar{q} \to V$ transition spinorial structure, namely, of $\bar{u}'\gamma_\mu u \cdot V_\mu$ type. Being a mere analogy of $q\bar{q}\gamma$ vertex, this ansatz in fact corresponds neither to pure $S$ nor to pure $D$ wave state but rather to their certain mixture. Only in [11] the cases of $1S$ and $2S$ vector mesons were compared and the necessity of similar calculation for $D$ wave states was stressed. Such calculations however have been missing in literature until now.

In addition to purely theoretical needs, there are more issues that call upon a thorough analysis of the $D$-wave effects. For instance, different spin properties of the $S$- and $D$-wave production may resolve the long standing problem of the $D$-wave vs. $2S$-wave assignment for the $\rho'(1480)$ and $\rho'(1700)$ mesons (as well as the $\omega'$ and $\phi'$ mesons). Furthermore, the deuteron which is a spin–1 ground state in the $pn$ system is known to have a substantial $D$ wave admixture, which mostly derives from the tensor forces induced by pion exchange between nucleons. Recently, there has been much discussion [12] of the nonperturbative long-range pion exchange between light quarks and antiquarks in a vector meson, which is a natural source of the $S$-$D$ mixing in the ground state $\rho$ and $\omega$ mesons.

Motivated by these considerations, we undertook a derivation of a full set of helicity amplitudes for diffractive electroproduction of pure $S$ and $D$-wave $q\bar{q}$ systems for all flavors and small to moderate momentum transfer $\Delta_\perp$ within the diffraction cone.

The structure of this thesis is following. In the next Chapter we develop a QCD–motivated formalism of pure $S$ and $D$ vector meson treatment. In Chapter 3 a thorough and detailed derivation of vector meson production amplitudes is given. In Chapter 4 we continue our analysis in the case of heavy quarkonia and discuss the most eye-catching differences between $S$

and $D$ wave production amplitudes. In Chapter 5 we present some numerical results and finally we draw conclusions. In the course of calculations, we aimed at maximally full presentation of intermediate steps and results. Thus, we hope that the present work might also be helpful for anyone who intends to start his or her own calculation in this field. Some of the math–heavy calculations comprise the Appendix.

We would like to underline that this work sheds a new light on the Deep Inelastic Scattering as a means of hadron structure investigation. Indeed, one is accustomed to using DIS as a probe of the proton (i.e. target) spin structure. We demonstrate here that it is a powerful tool for studying internal spin structure of a *vector meson* as well. To this point, our work reflects only a few steps in this promising and still not fully explored domain.

All the results given in this thesis were derived by the author. The only exception was the results shown in Fig.10, which were calculated by I.Akushevich, Inst. of High Energy Phys., Misnk . The majority of the results derived in this thesis have been published in [13] and presented as talks in [14, 15].

# 2 Description of a vector meson

In this section we first introduce the vector meson light cone wave function (LCWF) and show how it emerges in diagrammatic calculations. Then, describing $S$ and $D$ wave type vector particles, we give at once expressions for $S$ and $D$ wave vector meson spinorial structures, which we then prove by computing the normalization condition for LCWF. Finally, we also calculate $V \to e^+e^-$ decay constants to be used afterwards.

## 2.1 Bound states in QFT

While describing particle motion in non-relativistic Quantum Mechanics, one usually deals with a configuration space particle wave function, which is a good description because the number of particles is conserved. So, when one has a system of particles and shows that the wave function corresponding to their relative motion descreases at large relative distances at least exponentially, one can speak of a bound state.

In Quantum Field Theory (QFT) this approach needs an update, since the field function becomes an operator in Fock space. Besides, since a bound state always implies the presence of interaction, the projection of a physical bound state onto the Fock space of *free, non–interacting, plane-wave* state vectors has a rather complicated structure:

$$|V_{phys}\rangle = c_0|q\bar{q}\rangle + c_1|q\bar{q}g\rangle + c_2|q\bar{q}gg\rangle + c_3|q\bar{q}q\bar{q}\rangle + ... \tag{2}$$

We emphasize that in this decomposition quarks and gluons are assumed free, i.e. **on mass shell**. Coefficients $c_i$ can be called 'wave functions' of the given projection of a physical vector meson, with $|c_i|^2$ being the probability of finding a vector meson in a given state.

## 2.2 LCWF and vertex factor

Let us now outline how a wave function of a bound state appears in the diagrammatic language.

In the non-relativistic quantum mechanics, the two-particle bound state problem can be immediately reformulated as a problem for one particle of reduced mass $\mu$, moving in the external potential. This reformulation allows one to split the wave function into two factors: the wave function of the motion of the composite particle as whole and the wave function corresponding to the internal motion of constituents. The former part factors out trivially, while the latter wave function obeys the following Schodinger equation

$$\left[\frac{\hat{p}^2}{2\mu} + V(r)\right]\psi(r) = E\psi(r). \tag{3}$$

Since the wave function $\psi(r)$ and the interaction operator $V(r)$ exhibit good infinity behavior, one can rewrite this equation in the momentum representation

$$\frac{p^2}{2\mu}\psi(p) + \frac{1}{(2\pi)^3}\int d^3k V(k)\psi(p-k) = E\psi(p);$$

$$\left(\frac{p^2}{m} - E\right)\psi(p) = -\frac{1}{(2\pi)^3}\int d^3k V(k)\psi(p-k). \tag{4}$$

In this notation, this equation can be viewed as a homogeneous non-relativistic Bethe-Salpeter equation for the wave function $\psi(p)$ that describes the relative motion of constituents inside a composite particle.

Let us now introduce

$$\Gamma(p) \equiv \left(\frac{p^2}{m} - E\right)\psi(p) \tag{5}$$

Then Eq.(4) can be rewritten as

$$\Gamma(p) = -\frac{1}{(2\pi)^3}\int d^3k V(k)\frac{1}{\frac{(p-k)^2}{m} - E}\Gamma(p-k) \tag{6}$$

This equation has an absolutely straightforward diagrammatic interpretation (Fig.2). One sees that $\Gamma(p)$ stands for bound-state $\to$ constituents transition vertex, with $p$ being the relative momentum of the constituents, factor $1/[\frac{(p-k)^2}{m} - E]$ describes propagation of $q\bar{q}$ pair and $V(k)$ stands for the interaction between constituents. Of course, the kinetic energy $p^2/2\mu \neq E$, the total energy, which is in fact negative, so no pole arises in the propagator.
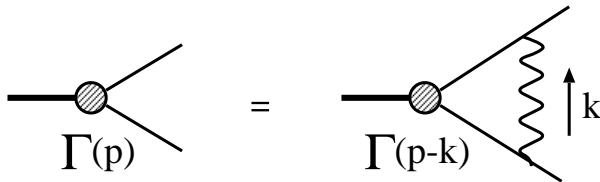


Figure 2: The diagrammatic interpretation of the integral equation for vertex function $\Gamma(p)$ ($p$ is the relative constituents momentum).

In the relativistic case, i.e. in QFT, it is not clear *a priori* whether the whole picture that involves somehow defined wave function and representation of the vector meson as free non-interacting constituents would work at all. So, in our approach we will be aiming at introducing an appropriately defined wave function and demonstrating that hard processes involving vector mesons can be expressed in terms of expectation values of $q\bar{q}$ amplitudes between wave functions, i.e. we intend to treat a hard process in a *probabilistic, quantum mechanics-like manner*.

In the following we will show that this program succeeds. Namely, we will introduce the *radial* wave function of the $q\bar{q}$ state of a vector meson as

$$\psi(q) \equiv \frac{\Gamma(q)}{M^2 - m_V^2} \tag{7}$$

(the angular dependence of the wave function will be treated separately, see Sect.2.4) Here $\Gamma(q)$ is the vertex factor, $M^2$ is the eigenvalue of the relativistic kinetic operator of the on mass shell $q\bar{q}$ state and $m_V^2$ is eigenvalue of the total relativisitic Hamiltonian, which is of course equal to the mass of the vector meson squared. Then, during an *accurate and honest* analysis of a hard process Feynman diagrams, we will always make sure that wave function (7) automatically appears in calculations and *the rest* looks the same as if both fermions were on mass shell. If we see that fermion virtualities modify the results, or if different Fock states mix during hard interactions of the vector meson, it would signal the invalidity of the free particle parton language and consequenly the breakdown of the whole approach. This restriction must always be taken into account when obtaining and interpreting the parton model-based results.

## 2.3 Light cone formalism

The term "light cone approach" to high–energy process calculations can have different meanings. Some prefer to re-formulate the whole QFT within light cone dynamics, introduce light cone quantization and derive light cone Feynman rules (on Light Cone Field Theory see [16, 17]). However, one should keep in mind that even within the usual QFT the light cone formalism can be freely used as a means to greatly simplify intermediate calculations. This is exactly the way we will use it.

It was noted long ago [18] that the calculation of a high energy collision is simplied if one decomposes all momenta in terms of light cone $n_+^\mu, n_-^\mu$ and transversal components, which we will always mark with the vector sign over a letter (so called Sudakov's decomposition):

$$n_+^\mu = \frac{1}{\sqrt{2}}(1, \vec{0}, 1) \,; \quad n_-^\mu = \frac{1}{\sqrt{2}}(1, \vec{0}, -1) \,; \quad (n_+ n_-) = 1 \,, \ (n_+ n_+) = (n_- n_-) = 0$$
$$p^\mu = p_+ n_+^\mu + p_- n_-^\mu + \vec{p}^{\,\mu} \,; \quad p^2 = 2p_+ p_- - \vec{p}^{\,2} \,. \tag{8}$$

Indeed, imagine two high energy particles colliding with momenta $p^\mu$ and $q^\mu$ respectively and equal masses $m$. Then one can choose such a frame of reference that in the Sudakov's decomposition

$$p^\mu = p_+ n_+^\mu + p_- n_-^\mu + \vec{p}^{\,\mu} \,,$$
$$q^\mu = q_+ n_+^\mu + q_- n_-^\mu + \vec{q}^{\,\mu}$$

quantities $p_-$ and $q_+$ are large $p_-, q_+ \gg m$ while $p_+ = (\vec{p}^{\,2} + m^2)/(2p_-)$ and $q_- = (\vec{q}^{\,2} + m^2)/(2q_+)$ are small. The total energy squared of these two particles will be defined as

$$s \equiv 2q_+ p_- \,. \tag{9}$$

Note that our definition of $s$ is somewhat different from the more familiar one $(p+q)^2$ by terms $\propto m^2, \vec{p}^{\,2}$. However, it is not of any imporatnce for us, since in the course of all calculations we will keep track only of the highest power $s$ contributions, i.e. everything will be calculated in the leading power $s$ approximation.
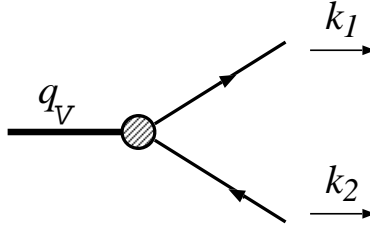


Figure 3: Kinematics of $V \to q\bar{q}$ vertex on the light cone. Vector meson momentum $q_V$ is taken incoming, constituents momenta are outgoing.

Let us now go further and examine the kinematics of a typical $q\bar{q}V$ vertex (Fig.3). The Sudakov's decomposition of all momenta reads:

$$q_V^\mu = q_{V+} n_+^\mu + q_{V-} n_-^\mu \,;$$
$$k_1^\mu = k_{1+} n_+^\mu + k_{1-} n_-^\mu + \vec{k}^{\,\mu} = z q_{V+} n_+^\mu + y q_{V-} n_-^\mu + \vec{k}^{\,\mu} \,;$$
$$k_2^\mu = k_{2+} n_+^\mu + k_{2-} n_-^\mu - \vec{k}^{\,\mu} = (1-z) q_{V+} n_+^\mu + (1-y) q_{V-} n_-^\mu - \vec{k}^{\,\mu} \tag{10}$$

so that
$$q_V^2 = 2q_{V+}q_{V-} = m_V^2 ; \quad k_1^\mu + k_2^\mu = q_V^\mu ; \quad k_i^2 \neq m^2 , \tag{11}$$

i.e. quarks can be off mass shell. Now let us introduce momenta $k_i^*$, which would correspond to on mass shell fermions. The only component in $k_i$ subject to modification is $k_{i-}$ component, or absolutely equivalently, the energy. Large $k_{i+}$ components are insensitive to (reasonable) quark virtuality variations. So, to obtain the on mass shell momenta, one has to replace

$$k_{i-} = \frac{k_i^2 + \vec{k}^2}{2k_{i+}} \to k_{i-}^* = \frac{m^2 + \vec{k}^2}{2k_{i+}} . \tag{12}$$

Then the 4-vector
$$q^\mu = k_1^{*\mu} + k_2^{*\mu} \tag{13}$$

squared is equal to

$$M^2 = q^2 = 2q_+q_- = 2q_{V+}\left(k_{1-}^* + k_{2-}^*\right) = \frac{\vec{k}^2 + m^2}{z(1-z)} . \tag{14}$$

And again we emphasize that the *Feynman invariant mass* (i.e. the total 4-momentum squared) of the virtual quark-antiquark pair is $m_V^2$. The quantity $M^2$ is the invariant mass of the free, non-interacting $q\bar{q}$ state (see 7). However, it is precisely $M$, not $m_V$ that will govern the hard interaction of $q\bar{q}$ pair with gluons.

Finally, it is useful to introduce the relative momentum of free $q\bar{q}$ system:

$$2p_\mu = (k_1^* - k_2^*)_\mu . \tag{15}$$

Then, trivial algebra leads to

$$M^2 = 4m^2 + 4\mathbf{p}^2 ; \quad p^2 = -\mathbf{p}^2 ; \quad (pq) = 0 , \tag{16}$$

where $\mathbf{p}$ is the 3–dimensional relative momentum in the $q\bar{q}$ pair rest frame of reference. Its components are

$$\mathbf{p} = (\vec{p}, p_z) ; \quad \vec{p} = \vec{k} ; \quad p_z = \frac{1}{2}(2z - 1)M . \tag{17}$$

## 2.4 Spin structure of a vector particle

Let us start with a well known example of a deuteron, which is a non-relativistic analogy of a vector meson: they are both vector particles built up of two fermions. To have the correct $P$-parity, proton and neutron must sit in the spin–triplet state, thus leaving us with two possible values of their angular momenta: $L = 0$ and 2.

In the conventional non-relativistic language one describes the spin-angular coupling by the Clebsh-Gordan technique. The non-relativistic Feynman diagram calculations can be best performed in an alternative approach. Here a deuteron, being a vector particle, is described by a 3 dimensional polarization vector $\mathbf{V}$. So, while calculating high energy processes involving $d \to pn$ transitions, one can use the following spin structure of deuteron-nucleon-nucleon vertex:

$$\phi_n^+ \, \mathbf{\Gamma} \, \phi_p \cdot \mathbf{V} \tag{18}$$

Since both nucleons can be treated on mass shell, only two terms enter $\Gamma_i$, which can be written as:

$$\phi_n^+ \left[ u(p)\sigma^i + w(p)(3p^i p^j - \delta^{ij} p^2)\sigma^j \right] \phi_p \cdot V^i \tag{19}$$

Here $\sigma^i$ are Pauli matrices and $\mathbf{p}$ is the relative proton–neutron momentum. One immediately recognizes here spin structures corresponding to $pn$ pair sitting in $S$ and $D$ waves respectively. In particular, squaring the above expression gives

$$
\begin{aligned}
&(\mathbf{VV}^*) \quad \text{for } |S|^2 \\
&3(\mathbf{pV})(\mathbf{pV}^*) - (\mathbf{VV}^*)\mathbf{p}^2 \quad \text{for } SD \text{ interference} \\
&3\mathbf{p}^2(\mathbf{pV})(\mathbf{pV}^*) + (\mathbf{VV}^*)\mathbf{p}^4 \quad \text{for } |D|^2
\end{aligned} \tag{20}
$$

Now, let us go relativistic and turn to vector mesons. The polarization state of a vector particle is described by a four-vector $V_\mu$. Therefore, a general form of $q\bar{q}V$ vertex has the form

$$\bar{u}'\Gamma_\mu u \cdot V_\mu \cdot \Gamma(p) ,$$

where $\Gamma(p)$ is the familiar vertex factor. Up to now, it has been customary in literature to choose the simplest form of the spinorial structure $\Gamma_\mu$:

$$\bar{u}'\gamma_\mu u \cdot V_\mu \cdot \Gamma(p) . \tag{21}$$

However, one must admit that (21) is simply an analogy of $q\bar{q}\gamma$ vertex and does not reflect the true internal structure of a vector meson. It is known [19] that the correct spinorial structure corresponding to pure the $S$ wave $q\bar{q}$ state reads

$$S_\mu = \gamma_\mu - \frac{2p_\mu}{M + 2m} = \left( g_{\mu\nu} - \frac{2p_\mu p_\nu}{m(M + 2m)} \right) \gamma_\nu \equiv \mathcal{S}_{\mu\nu}\gamma_\nu . \tag{22}$$

It is implied here that spinorial structures are inserted between *on mass shell spinors* in accordance with our principal guideline (see discussion in Sect.2.2).

Once $S$ wave spinorial structure is established, the expression for $D$ wave can be obtained by contracting $S$ wave with the symmetric traceless tensor of rank two $3p_i p_j - \delta_{ij}\mathbf{p}^2$, rewritten in the Lorenz notation. To do so, one should replace

$$p_i \rightarrow p_\mu ; \quad \delta_{ij} \rightarrow -g_{\mu\nu} + \frac{q_\mu q_\nu}{M^2}$$

(in the $q\bar{q}$ pair rest frame of reference $q_\mu = (M, 0, 0, 0)$). However, since $q_\mu$ inserted between on mass shell spinors gives zero due to the Ward identity, one obtains the required tensor in the form $3p_\mu p_\nu + g_{\mu\nu}\mathbf{p}^2$. Its contraction with $\mathcal{S}_\mu$ yields

$$D_\mu = (3p_\mu p_\nu + g_{\mu\nu}\mathbf{p}^2) \cdot \mathcal{S}_{\nu\rho}\gamma_\rho = \mathbf{p}^2\gamma_\mu + (M+m)p_\mu = \left( \mathbf{p}^2 g_{\mu\nu} + \frac{M+m}{m}p_\mu p_\nu \right) \gamma_\nu \equiv \mathcal{D}_{\mu\nu}\gamma_\nu . \tag{23}$$

We will prove below that structures (22), (23) after being squared indeed perfectly reproduce (20), i.e. they indeed correspond to pure $S$ and $D$ waves.

The quantities $\mathcal{S}_{\mu\nu}$ and $\mathcal{D}_{\mu\nu}$ used in (22), (23) have the meaning of $S/D$ wave projectors, which will be used in all subsequent calculations. Namely, all calculations will be at first performed for the naive $q\bar{q}V$ vertex (21) and then we will apply the projector technique to obtain expressions for $S$ and $D$ wave states.

## 2.5 Vector meson LCWF normalization

Before tackling the diffractive vector meson production process, we first should have a prescription of normalization of the vector meson wave function.

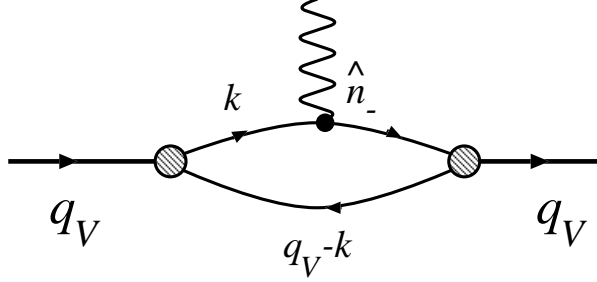### 2.5.1 Naive $q\bar{q}V$ vertex



Figure 4: Diagram used for normalizing the vector meson LCWF. The amplitude of this diagrams is set equal to $2q_+i$.

A natural way to normalize the wave function of a composite system is to put the amplitude given by this diagram in Fig.4 equal to $2q_+i$. Here extra leg carries zero momentum but couples to the fermion line as $\gamma_\mu n^\mu_-$. Note that for a charged composite particle (a deuteron) this is precisely setting the electric formfactor equal to unity in the soft photon limit.

As described above, we first treat $q\bar{q}V$ vertex as $\bar{u}'\gamma_\mu u \cdot \Gamma(p)$. In this case the general expression for this amplitude is

$$A = \frac{(-1)}{(2\pi)^4}N_c \cdot \int d^4k \frac{Sp\{i\hat{V}_1\Gamma \cdot i(\hat{k}-\hat{q}_V+m) \cdot i\hat{V}_2^*\Gamma^* \cdot i(\hat{k}+m) \cdot i\hat{n}_- \cdot i(\hat{k}+m)\}}{[k^2-m^2+i\epsilon] \cdot [k^2-m^2+i\epsilon] \cdot [(k-q_V)^2-m^2+i\epsilon]}$$

$$= \frac{N_c}{(2\pi)^4} \cdot \int d^4k \frac{|\Gamma|^2 Sp\{...\}}{[k^2-m^2+i\epsilon]^2[(k-q_V)^2-m^2+i\epsilon]}, \quad (24)$$

where $N_c = 3$ is a trivial color factor originating from the quark loop. We deliberately recognized $V_1$ and $V_2$ as distinct entities just to make sure later that such a loop is indeed diagonal in polarization states.

The first step is to rewrite this expression in terms of Sudakov's variables. As usual, one implements decomposition

$$k^\mu = zq_{V+}n^\mu_+ + yq_{V-}n^\mu_- + \vec{k}^\mu; \quad q_V^2 = 2q_{V+}q_{V-} = m_V^2$$

and transforms

$$d^4k = \frac{1}{2}m_V^2 d^2\vec{k}dydz.$$

Now we note that vertex functions $\Gamma$ do not depend on $y$ (and neither does the trace, as will be shown later), so we can immediately perform the integrations over $y$ by means of Cauchy theorem. Indeed, since the integral

$$\int_{-\infty}^{\infty} dy \frac{1}{[yzm_V^2 - (\vec{k}^2+m^2)+i\epsilon]^2} \frac{1}{[(1-y)(1-z)m_V^2 - (\vec{k}^2+m^2)+i\epsilon]}, \quad (25)$$

is convergent and has good infinity behavior, one can close the integration contour in the most convenient way. To do so, one should analyze the position of all poles on the complex $y$ plane:

$$y_{1,2} = \frac{\vec{k}^2 + m^2}{zm_V^2} - \frac{i\epsilon}{zm_V^2}; \quad y_3 = 1 - \frac{\vec{k}^2 + m^2}{(1-z)m_V^2} + \frac{i\epsilon}{(1-z)m_V^2}.$$

One sees that if $z < 0$ or $z > 1$, *all* poles lie on the same side of the real axis in the complex $y$ plane, which leads to zero contribution. The contribution that survives comes from region $0 < z < 1$, which has in fact a simple physical meaning: all constituents must move in the same direction. In this region, we close the integration contour through the upper half-plane and take a residue at $y = y_3$. Physically, it corresponds to putting the antiquark on mass shell. After this procedure, one gets for (25):

$$-\frac{2\pi i}{(1-z)m_V^2}\frac{1}{[yzm_V^2 - (\vec{k}^2 + m^2) + i\epsilon]^2}\bigg|_{y=y_3} = -\frac{2\pi i}{(1-z)m_V^2}\frac{(1-z)^2}{[\vec{k}^2 + m^2 - z(1-z)m_V^2]^2}$$
$$= -\frac{2\pi i}{m_V^2}\frac{1}{z^2(1-z)}\frac{1}{[M^2 - m_V^2]^2}.$$

One immediately recognizes here the same two-particle propagator as in (7). Therefore, the equation for the amplitude reads

$$A = i\frac{N_c}{(2\pi)^3}\cdot\int d^2\vec{k}\frac{dz}{z^2(1-z)}\cdot|\psi|^2\cdot\left(-\frac{1}{2}Sp\{...\}\right). \tag{26}$$

Now we turn to the trace calculation. To do this, we will first show that thanks to the presence of $\hat{n}_-$ vertex, *both constituents* indeed can be treated in the numerator algebra as if they were on mass shell. Indeed, applying the Sudakov decomposition to the $\gamma$ matrix, one has

$$\gamma^\mu = \gamma_+ n_+^\mu + \gamma_- n_-^\mu + \vec{\gamma}^\mu;$$
$$\gamma_+ = \hat{n}_- = \frac{1}{\sqrt{2}}(\gamma_0 + \gamma_3), \quad \gamma_- = \hat{n}_+ = \frac{1}{\sqrt{2}}(\gamma_0 - \gamma_3).$$

Now let's decompose the propagator numerator of the constituent, to which this $\hat{n}_-$ leg couples:

$$\hat{k} + m = k_+\gamma_- + k_-\gamma_+ - \vec{k}\vec{\gamma} + m \tag{27}$$

and rewrite it using notation of (10),(12) as

$$\hat{k} + m = k_+\gamma_- + k_-^*\gamma_+ - \vec{k}\vec{\gamma} + m + (k_- - k_-^*)\gamma_+ = \hat{k}^* + m + \frac{k^2 - m^2}{2k_+}\gamma_+. \tag{28}$$

In other words, we expressed the virtual quark propagator as the sum of *on shell* quark propagator and an additional "instantaneous interaction" term. However, since $\hat{n}_-$ is inserted between two $(\hat{k} + m)$ factors, this item does not work due to identity $\gamma_+\gamma_+ = 0$. The net result is that *wherever $\hat{n}_-$ appears, both constituents can be treated on mass shell in the trace calculation.* This observation is very important for us, since, as we remember, it validates the whole approach.

Having established this property, we can now easily calculate the trace. In our case, the easiest way is to do it covariantly, without involving further the Sudakov technique. Since quarks in numerator can be treated on mass shell, we first note that

$$(\hat{k} + m)\hat{n}_-(\hat{k} + m) = 2(k^* n_-)(\hat{k}^* + m)$$

so that

$$-\frac{1}{2}Sp\{...\} = -zq_+ Sp\{\hat{V}_1(\hat{k}^* - \hat{q} + m)\hat{V}_2^*(\hat{k}^* + m)\} = -2zq_+ \left[M^2(V_1V_2^*) + 4(V_1p)(V_2^*p)\right],$$

where $p$ is the relative quark-antiquark momentum [see (16)]. Note that in the antiquark propagator we replaced $\hat{k} - \hat{q}_V \to \hat{k}^* - \hat{q}$, since the antiquark is now put on mass shell. Besides, we explicitly used here gauge condition $(qV) = 0$, which means that polarization vectors must be written for *on mass shell* $q\bar{q}$ *pair*, not the vector meson, — another important consequence of our approach. Substituting this into (26), one gets

$$1 = \frac{N_c}{(2\pi)^3} \int d^2\vec{k}\frac{dz}{z(1-z)}|\psi|^2 \left[-M^2(V_1V_2^*) - 4(V_1p)(V_2^*p)\right]. \tag{29}$$

A prominent feature of this equation is the orthogonality of $V_L$ and $V_T$ polarization states — the necessary condition for any normalization prescription.

The next step is to realize that the integral can be cast in the form of $d^3\mathbf{p}$ integration by means of

$$\frac{dz}{z(1-z)}d^2\vec{k} = \frac{4}{M}dp_z d^2\vec{p} = \frac{4}{M}d^3\mathbf{p}.$$

Tus, the final expression for normalization condition is

$$1 = \frac{N_c}{(2\pi)^3} \int d^3\mathbf{p}\frac{4}{M}|\psi|^2[-M^2(V_1V_2^*) - 4(V_1p)(V_2^*p)]. \tag{30}$$

We see that the expression being integrated is explicitly spherically non-symmetric, which is a manifestation of a certain $D$ wave admixture. Thus we now apply projector technique to obtain results for $S$ and $D$ wave states.

### 2.5.2 Normalization for $S$ wave vector meson

The correct expressions for pure $S/D$ type vertices can be readily obtained with the aid of projector technique. Namely, to obtain an expression for $S$ wave, replace

$$V_\mu \to V_\nu \mathcal{S}_{\nu\mu}. \tag{31}$$

Such a replacement for $V_1$ leads to

$$-M^2(V_1V_2^*) - 4(V_1p)(V_2^*p) \Rightarrow -M^2(V_1V_2^*) - \frac{4M}{M+2m}(V_1p)(V_2^*p)$$

Then, one applies the same replacement to $V_2^*$ to obtain

$$-M^2(V_1V_2^*) - \frac{4M}{M+2m}(V_1p)(V_2^*p) \Rightarrow -M^2(V_1V_2^*).$$

Therefore, the answer for $S$ wave states reads

$$\boxed{1 = \frac{N_c}{(2\pi)^3} \int d^3\mathbf{p} \; 4M|\psi^S(\mathbf{p}^2)|^2}$$

(32)

which is manifestly spherically symmetric.

### 2.5.3  Normalization for $D$ wave vector meson

Results for $D$ wave states are derived in the same way. The replacements $V_\mu \to V_\nu \mathcal{D}_{\nu\mu}$ lead to

$$- M^2\mathbf{p}^4(V_1 V_2^*) + 3M^2\mathbf{p}^2(V_1 p)(V_2^* p) \,.$$

(33)

After angular averaging

$$\langle p_i p_j \rangle \to \frac{1}{3}\mathbf{p}^2 \delta_{ij},$$

one gets the normalization formula for $D$ wave state:

$$\boxed{1 = \frac{N_c}{(2\pi)^3} \int d^3\mathbf{p} \; 8M\mathbf{p}^4|\psi^D(\mathbf{p}^2)|^2}$$

(34)

Several remarks are in order. First, $S$ wave $\to D$ wave transitions are forbidden. Indeed, such an amplitude will be proportional to

$$- M^2[\mathbf{p}^2(V_1 V_2^*) + 3(V_1 p)(V_2^* p)] \,.$$

(35)

which vanishes after angular integration. Then, we emphasize that the structure of results (32), (33), (35) is absolutely identical to Eq.(20). This fact can be viewed as the *proof* that spinorial structures (22), (23) indeed correspond to pure $S$ and $D$ wave states.

## 2.6  Decay constant
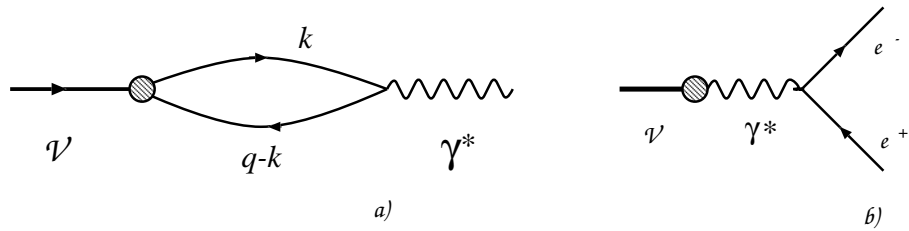


Figure 5: Normalizing LCWF to $\Gamma(V \to e^+e^-)$ decay width: (a) the diagram for $V \to \gamma^*$ transition, (b) the diagram for $V \to e^+e^-$ decay.

An additional normalization condition consists in relating the vector meson wave function to the experimentally measurable physical quantity — $V \to e^+e^-$ decay width (Fig.5). The

loop at Fig.5a describes transition $V \to \gamma^*$ and enters the amplitude of the decay $V \to e^+e^-$ (Fig.5b). Let us define the decay constant via relation

$$\mathcal{A} = i\langle 0|J_\mu^{em}|V\rangle = -if_V c_V \sqrt{4\pi\alpha} V_\mu. \tag{36}$$

So defined $f_V$ has dimension $\dim[f_V] = m^2$. The quantity $c_V$ reflects the flavor content of a vector meson (in the previous calculations it simply gave unity) and is equal to

$$c_V = \frac{1}{\sqrt{2}}, \frac{1}{3\sqrt{2}}, -\frac{1}{3}, \frac{2}{3} \tag{37}$$

for $\rho, \omega, \phi, J/\psi$ mesons correspondingly.

Knowing that such a loop does not mix polarization states, we can multiply both sides of eq.(36) by $V^*$ and get the expression

$$if_V = \frac{(-1)}{(2\pi)^4} N_c \cdot \int d^4k \frac{Sp\{i\hat{V}^* \cdot i(\hat{k}+m) \cdot i\hat{V}\Gamma \cdot i(\hat{k}-\hat{q}_V+m)\}}{(k^2-m^2+i\epsilon) \cdot ((k-q_V)^2-m^2+i\epsilon)}. \tag{38}$$

Calculations similar to the above normalization condition derivation yield (for the naive type of vertex)

$$f_V = \frac{N_c}{(2\pi)^3} \cdot \int \frac{dz}{z(1-z)} d^2\vec{k} \ \psi_V[-M^2(VV^*) - 4(Vp)(V^*p)]. \tag{39}$$

Applying now the projector technique, one gets in the case of $S$ states (after proper angular averaging)

$$\boxed{f^{(S)} = \frac{N_c}{(2\pi)^3} \cdot \int d^3\mathbf{p} \ \psi_S \frac{8}{3}(M+m)} \tag{40}$$

and in the case of $D$ wave states

$$\boxed{f^{(D)} = \frac{N_c}{(2\pi)^3} \cdot \int d^3\mathbf{p} \ \psi_D \frac{32}{3} \frac{\mathbf{p}^4}{M+2m}.} \tag{41}$$

Finally, one can write down the expression for the decay width in terms of $f_V$:

$$\Gamma(V \to e^+e^-) = \frac{1}{32\pi^2 m_V^2} \cdot \frac{m_V}{2} 4\pi|A|^2 = \frac{4\pi\alpha^2}{3m_V^3} \cdot f_V^2 c_V^2. \tag{42}$$

This formula can be used to extract the numerical value of $f_V$ from experimental data.

## 2.7  Ansatz for LCWF

In order to perform some model evaluations, one should fix a particular form for the vector meson wave function. We will give just two examples often used in calculations: Coulomb–type and oscillator type wave functions.

### 2.7.1 Coulomb wave functions

As one can see from Eqs.(32) and (34), a LCWF should contain $M$ dependence in form of $M^{-1/2}$ (the normalization condition for non-relativistic wave function deals with $\int d^3 p |\psi_{NR}|^2$ ). So, in this ansatz the normalized wave functions read

$$
\begin{aligned}
\psi_{1S}(\mathbf{p}^2) &= \frac{c_1}{\sqrt{M}} \frac{1}{(\mathbf{p}^2 + \alpha_1^2)^2}; \\
\psi_{2S}(\mathbf{p}^2) &= \frac{c_2}{\sqrt{M}} \frac{(\mathbf{p}^2 - \alpha_2^2)}{(\mathbf{p}^2 + \alpha_2^2)^3}; \\
\psi_D(\mathbf{p}^2) &= \frac{c_D}{\sqrt{M}} \frac{1}{(\mathbf{p}^2 + \alpha_D^2)^4}.
\end{aligned}
\tag{43}
$$

with normalization constants to be determined from Eqs.(32) and (34). Here parameters $\alpha_i$ are connected to the size of a bound system: in the coordinate representation $\psi_i \propto \exp(-r\alpha_i)$. For usual Coulomb functions $3\alpha_D = 2\alpha_2 = \alpha_1 = 1/R_{Bohr}$, where $R_{Bohr}$ is the Bohr radius. However, this relation should be treated with care in the case of $q\bar{q}$ quarkonia, where the quark-antiquark potential is quite complicated and therefore $\alpha_i$ should rather be considered as free parameters.

As an example, let's compute the ratio $f_D/f_{1S}$ with these wave functions in the non-relativistic limit, when $M \approx m_V \approx 2m$. It will be useful later in the analysis of heavy vector mesons.

$$
\frac{f_D}{f_S} = \sqrt{\frac{80}{9}} \sqrt{\frac{R_S^3}{R_D^3}} \cdot \frac{1}{m_V^2 R_D^2}.
\tag{44}
$$

Here $R = 1/\alpha$ is a typical size of a vector meson in a given state.

### 2.7.2 Oscillator type LCWF

In this ansatz one has

$$
\begin{aligned}
\psi_{1S} &= \frac{c_1}{\sqrt{M}} \exp\left(-\frac{\mathbf{p}^2 R_1^2}{2}\right); \\
\psi_{2S} &= \frac{c_2}{\sqrt{M}} \left(1 - \frac{2}{3}\mathbf{p}^2 R_2^2\right) \exp\left(-\frac{\mathbf{p}^2 R_2^2}{2}\right); \\
\psi_D &= \frac{c_D}{\sqrt{M}} \exp\left(-\frac{\mathbf{p}^2 R_D^2}{2}\right).
\end{aligned}
\tag{45}
$$

Note again that for purely oscillator potential one also has relation $R_D = R_1 = R_2$, which might not hold in our case, since the oscillator type potential is also a crude approximation of the true quark-antiquark interaction. A similar calculation for $f_D/f_S$ ratio yields

$$
\frac{f_D}{f_S} = \sqrt{\frac{160}{3}} \sqrt{\frac{R_S^3}{R_D^3}} \cdot \frac{1}{m_V^2 R_D^2}.
\tag{46}
$$

Note that the oscillator ansatz gives at least $\sqrt{6}$ times larger $f_D/f_S$ ratio. Therefore, one must admit that such model dependent calculations are plagued by a great deal of arbitrariness, which will inevitably affect the results.

# 3 Vector meson production amplitudes
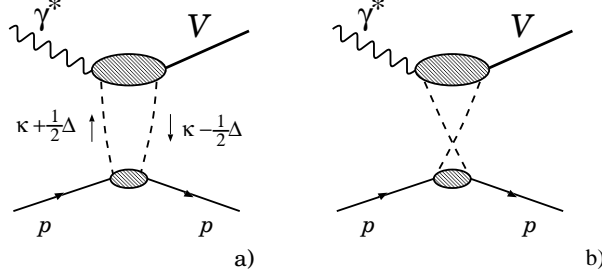
## 3.1 Preliminary notes



Figure 6: The QCD–inspired diagrams for $\gamma^* p \to V p$ process with two gluon $t$–channel. Only Diagr.(a) does contribute to the imaginary part of amplitudes.

Having set up the notation and defined and described a vector meson by itself, we are now ready to evaluate the full set of amplitudes of its off-forward virtual diffractive photoproduction.

In the pQCD motivated approach to this process the pomeron exchange is viewed as a two-gluon exchange as it is shown in Fig.6a. Using the scalarization procedure, we will split the diagram into 2 pieces and will treat each of them separately. The upper blob describes the pomeron-assisted transition of the virtual photon into a vector meson. In the perturbative QCD approach, which is legitimate here due to the presence of the relevant hard scale $\overline{Q}^2 = m_q^2 + z(1-z)Q^2$, the $q\bar{q}$ fluctuation of the virtual photon interacts with two hard gluons and then fuses to produce a vector meson. This interaction is described by four diagrams given in Fig.7, with all possible two-gluons attachments to $q\bar{q}$ pair taken into account. All of them are equally important and needed for maintaining gauge–invariance and color transparency. The latter property means that in the case of very soft gluons the upper blob must yield zero, for the $q\bar{q}$ pair is colorless.

The lower part of the general diagram Fig.6a is of course not computable in pQCD. The physically meaningful procedure is to relate it to the experimentally measurable gluon density. To do so, we will first calculate this lower blob in the Born approximation and then give a prescription how to introduce the unintergrated gluon density. In the course of this procedure, we will neglect in the intermediate calculations proton off-forwardness and take it into account only at the very end, as a certain factor to the unintegrated gluon density.

## 3.2 Notation and helicity amplitudes

In our calculation we will use the following Sudakov's decomposition (see also Fig.8a)

$$
\begin{aligned}
k_\mu &= -y p_\mu{}' + z q_\mu{}' + \vec{k}_\mu \,; \\
\kappa_\mu &= \alpha p_\mu{}' - \beta q_\mu{}' + \vec{\kappa}_\mu \,; \\
\Delta_\mu &= \delta p_\mu{}' + \sigma q_\mu{}' + \vec{\Delta}_\mu
\end{aligned}
\tag{47}
$$

Here $k$ and $\kappa$ are momenta that circulate in the quark and gluon loops respectively; $\Delta$ is the momentum transfer. Vectors $p_\mu{}'$ and $q_\mu{}'$ denote the light-cone momenta: they are related to
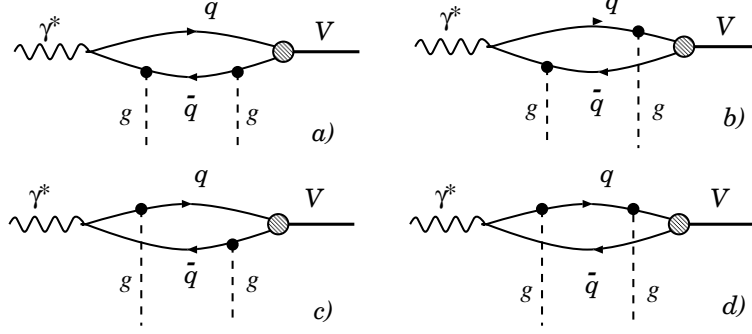
Figure 7: The content of the upper blob in Fig.6a in the pQCD approach. The true vector meson internal structure is approximated by $q\bar{q}$ Fock state.
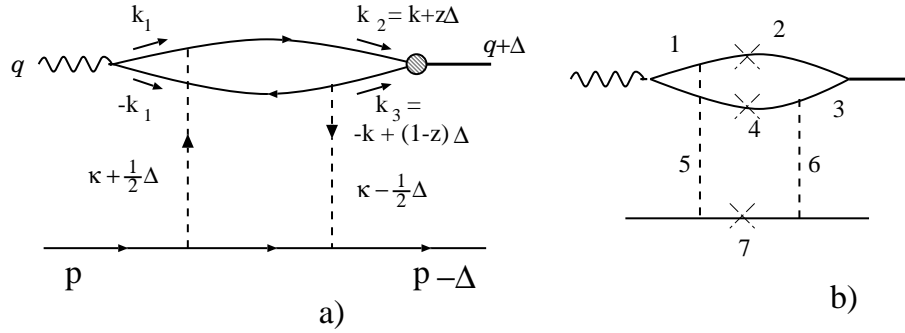


Figure 8: (a): A particularly useful convention of the loop momenta (only transverse components of quark momenta are shown). (b): the propagator notation used while calculating denominators. The crosses denote on mass shell particles.

the proton and virtual photon momenta as

$$p_\mu = p_\mu' + \frac{m_p^2}{s}q_\mu'; \quad q_\mu = q_\mu' - xp_\mu'; \quad q'^2 = p'^2 = 0; \quad x = \frac{Q^2}{s} \ll 1; \quad s = 2(p'q'). \quad (48)$$

As it was mentioned in the Introduction, the condition $x \ll 1$ is necessary to speak about diffractive processes. The longitudinal momentum transfer can be readily found from kinematics (see Fig.6). To the higher power $s$ terms it reads

$$m_p^2 = p^2 = (p - \Delta)^2 = m_p^2 - 2(p\Delta) + \Delta^2; \quad \Rightarrow \quad \sigma = -\frac{\vec{\Delta}^2}{s} \; ;$$

$$m_V^2 = (q + \Delta)^2 = -Q^2 + 2(q\Delta) + \Delta^2 \quad \Rightarrow \quad \delta = x + \frac{m_V^2 + \vec{\Delta}^2}{s} \; . \quad (49)$$

The final vector meson momentum reads:

$$q_{V\mu} = q_\mu' + \frac{m_V^2 + \vec{\Delta}^2}{s}p_\mu' + \vec{\Delta}_\mu \; . \quad (50)$$

Finally, throughout the text transverse momenta will be marked by the vector sign as $\vec{k}$ and 3D vectors will be written in bold.

21

There are several possible helicity amplitudes in the transition $\gamma^*_{\lambda_\gamma} \to V_{\lambda_V}$. First of all, both photon and vector meson can be transversely polarized. The polarization vectors are

$$e_{T\mu} = \vec{e}_\mu \,; \quad V_{T\mu} = \vec{V}_\mu + \frac{2(\vec{\Delta}\vec{V})}{s}(p' - q')_\mu \,. \tag{51}$$

Note that we took into account the fact that the vector meson momentum has finite transverse component $\vec{\Delta}$. Then, the virtual photon can have the scalar polarization (which is often called longitudinal; we will use both terms) with polarization vector

$$e_{0\mu} = \frac{1}{Q}(q' + xp')_\mu \,. \tag{52}$$

Finally, the longitudinal polarization state of a vector meson is described by

$$V_{L\mu} = \frac{1}{M}\left(q_\mu{}' + \frac{\vec{\Delta}^2 - M^2}{s}p_\mu{}' + \vec{\Delta}_\mu\right) \,. \tag{53}$$

Note that, as we already mentioned, in the self-consistent approach we must take the *running polarization vector* for the longitudinal polarization state. It depends on $M$, not $m_V$, which reflects the fact that in our approach we first calculate the production of *an on-shell $q\bar{q}$ pair with* (whose dynamics is governed by $M$) and then projects it onto the physical vector meson. We stress that this projection will automatically arise in the course of usual Feynman diagram evaluation.

Thus, there are 5 different amplitudes:

$$\begin{aligned}
&L \to L \\
&T \to T \ (\lambda_\gamma = \lambda_V) \\
&T \to L \\
&L \to T \\
&T \to T \ (\lambda_\gamma = -\lambda_V)
\end{aligned} \tag{54}$$

The first two are helicity conserving amplitudes. They are dominant and almost insensitive to the momentum transfer $\vec{\Delta}$. The next two are single helicity flipping amplitudes. They are unavoidably proportional to $|\vec{\Delta}|$ in the combination $(\vec{e}\vec{\Delta})$ or $(\vec{V}^*\vec{\Delta})$ and would be vanishing for the strictly forward scattering. Finally, the last amplitude corresponds to the double helicity flip and will be proportional to $(\vec{e}\vec{\Delta})(\vec{V}^*\vec{\Delta})$.

## 3.3 General amplitude

We will take diagr.(c) at Fig.7 (it is shown in fig.8) as a generic diagram and perform a thorough analysis for it. It turns out that the other diagrams are calculated in the same fashion.

The general expression for the amplitude given by diagr.(c) reads:

$$iA = \int \frac{d^4k}{(2\pi)^4} \int \frac{d^4\kappa}{(2\pi)^4} \ \bar{u}'_p(-ig\gamma^{\nu'}t^{B'})i\frac{\hat{p} - \hat{\kappa}_1 + m_p}{\left[(p-\kappa)^2 - m_p^2 + i\epsilon\right]}(-ig\gamma^{\mu'}t^{A'})u_p$$

$$
\cdot (-i)\frac{g_{\mu\mu'}\delta_{AA'}}{\kappa_1^2 - \mu^2 + i\epsilon} \cdot (-i)\frac{g_{\nu\nu'}\delta_{BB'}}{\kappa_2^2 - \mu^2 + i\epsilon} \cdot c_V \cdot \Gamma^*
$$

$$
\cdot \frac{Sp\left\{ie\hat{e}\; i(\hat{k}_4 + m)\; (-ig\gamma^\nu t^B)\; i(\hat{k}_3 + m) i\hat{V}^*\; i(\hat{k}_2 + m)\; (-ig\gamma^\mu t^A)\; i(\hat{k}_1 + m)\right\}}{\left[k_1^2 - m^2 + i\epsilon\right]\left[k_2^2 - m^2 + i\epsilon\right]\left[k_3^2 - m^2 + i\epsilon\right]\left[k_4^2 - m^2 + i\epsilon\right]}
\tag{55}
$$

Here $c_V$ is the same as in (37) and $\Gamma$ is the familiar $q\bar{q} \to V$ vertex function. Note that we introduced 'gluon mass' $\mu$ in gluon propagators to account for confinement at a phenomenological level.

Let's first calculate the numerator.

## 3.4 Color factor

If we consider *strictly forward* gluon scattering off a single quark, we have

$$
\frac{1}{N_c}Sp\{t^{B'}t^{A'}\} \cdot \delta_{AA'}\delta_{BB'}Sp\{t^B t^A\} = \frac{1}{N_c}\frac{1}{2}\delta_{AB}\frac{1}{2}\delta_{AB} = \frac{1}{2}\frac{N_c^2 - 1}{2N_c} = \frac{1}{2}C_F = \frac{2}{3}
\tag{56}
$$

However, we should take into account that quarks are sitting inside a colorless proton, whose color structure is

$$
\psi_{color} = \frac{1}{\sqrt{6}}\epsilon^{abc}q^a q^b q^c
\tag{57}
$$

In this case there are two ways a pair of gluons can couple 3 quark lines (see Fig.9). In the first way both gluons couple to the same quark. Since the quark momentum does not change after these two interactions, the nucleon stays in the same state: $\langle N|N\rangle = 1$. In the second case gluon legs are attached to different quark lines, so that extra momentum $\kappa$ circulates between quarks, which gives rise to the factor $\langle N|\exp(i\kappa r_1 - i\kappa r_2)|N\rangle$, i.e. to the two-body formfactor. Therefore, for the lower line instead of

$$
\frac{1}{N_c}Sp\{t^B t^A\} = \frac{1}{N_c}\frac{1}{2}\delta_{AB}
\tag{58}
$$

one has

$$
\begin{aligned}
&\frac{1}{6}\epsilon^{abc}\left(3\delta_{aa'}\delta_{bb'}t_{cc''}^A t_{c''c'}^B + 6\delta_{aa'}t_{bb'}^A t_{cc'}^B\langle N|\exp(i\kappa r_1 - i\kappa r_2)|N\rangle\right)\epsilon^{a'b'c'}\\
=\; & Sp\{t^A t^B\} - Sp\{t^A t^B\}\langle N|\exp(i\kappa r_1 - i\kappa r_2)|N\rangle\\
=\; & \frac{1}{2}\delta_{AB}(1 - \langle N|\exp(i\kappa r_1 - i\kappa r_2)|N\rangle)\,.
\end{aligned}
\tag{59}
$$

Note also that a similar calculation for $N_c$ number of colors would yield the same result. Thus, the overall color factor is

$$
\frac{1}{2}C_F N_c V(\kappa) = 2V(\kappa) \equiv \frac{1}{2}C_F N_c(1 - \langle N|\exp(i\kappa r_1 - i\kappa r_2)|N\rangle)\,.
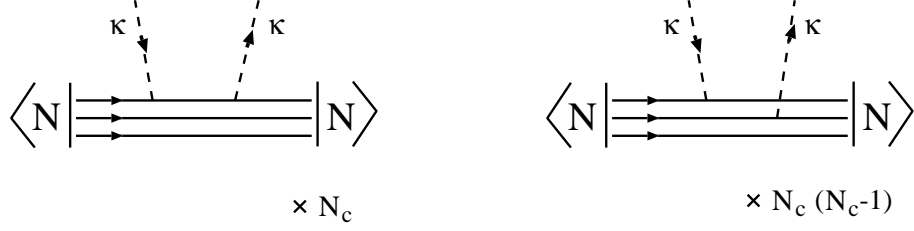\tag{60}
$$

Figure 9: The ways two glons can couple a colorless nucleon.

## 3.5 Scalarization of upper and lower parts

As known, the highest power $s$ contribution comes from so–called nonsense components of gluon propagator (density matrix) decomposition:

$$g_{\mu\mu'} = \frac{2p'_\mu q'_{\mu'}}{s} + \frac{2p'_\mu q'_{\mu'}}{s} + g^\perp_{\mu\mu'} \approx \frac{2p'_\mu q'_{\mu'}}{s}. \tag{61}$$

The lower (proton) line gives then

$$\bar{u}'(p) \cdot \hat{q}'(\hat{p} - \hat{\kappa}_1 + m_p)\hat{q}' \cdot u(p - \Delta) \tag{62}$$

To the highest power $s$ order, it can be rewritten as

$$\bar{u}'_p \hat{q}' \hat{p}' \hat{q}' u_p \Big|_{forward} = \frac{1}{2} Sp\{\hat{p}' \hat{q}' \hat{p}' \hat{q}'\} = s^2. \tag{63}$$

As we mentioned, the effect of off–forwardness (skewedness) will be taken into account later. So, combining all factors, one has for numerator of Eq.(55)

$$(4\pi\alpha_s)^2 \sqrt{4\pi\alpha_{em}} \ c_V \cdot \frac{1}{2} C_F N_c V(\kappa) \frac{4}{s^2} s^2 \cdot Sp\left\{\hat{e} \ (\hat{k}_4 + m) \ \hat{q}' \ (\hat{k}_3 + m) \ \hat{V}^* \ (\hat{k}_2 + m) \ \hat{q}' \ (\hat{k}_1 + m)\right\}$$

$$= (4\pi\alpha_s)^2 \sqrt{4\pi\alpha_{em}} \ c_V \cdot 2 C_F N_c V(\kappa) \cdot 2s^2 \cdot I^{(c)}(\gamma^* \to V). \tag{64}$$

Note that we factored out $2s^2$ from the trace because it will appear later in all trace calculations. So, the resulting expression for amplitude (55) looks like

$$A = \sqrt{4\pi\alpha_{em}} \ 4C_F N_c s^2 \ c_V \cdot \int \frac{d^4k}{(2\pi)^4} \int \frac{d^4\kappa}{(2\pi)^4} \cdot \frac{(4\pi\alpha_s)^2 V(\kappa)}{\left[(p - \kappa_1)^2 - m_p^2 + i\epsilon\right] [\kappa_1^2 - \mu^2 + i\epsilon] [\kappa_2^2 - \mu^2 + i\epsilon]}$$

$$\cdot \frac{\Gamma^* I^{(c)}(\gamma^* \to V)}{[k_1^2 - m^2 + i\epsilon] [k_2^2 - m^2 + i\epsilon] [k_3^2 - m^2 + i\epsilon] [k_4^2 - m^2 + i\epsilon]} \tag{65}$$

One can now immediately write similar expressions for the other three diagrams (Fig.7 a,b,d). Indeed, they will differ from Eq.(65) only by the last line: they will have different expressions for traces and propagator structures (i.e. the exact values for $k_i$.).

## 3.6 Denominator evaluation

Now we turn to the calculation of denominators. As usual, we implement Sudakov's decomposition (47) and make use of relation

$$d^4k = \frac{1}{2} s dy \, dz \, d^2\vec{k}.$$

The physical picture of the way we will do the resulting integrals is the following. We are interested only in the imaginary part of these diagrams. In fact, it can be shown that at the level of accuracy used here the diagram in Fig.6a gives rise only to the imaginary part of the amplitude. The real part is given by Fig.6b and can be readily found from analiticity (so that here is no need for additional calculations), however it turns out small due to smallness of pomeron intercept, so we will neglect it in our subsequent calculations.

The imaginary part is computed by setting three particles in the $s$-channel cut on mass shell (this is illustrated in Fig.8b). One way to do so is to apply Cutkosky rule to modify our expression. Another, more straightforward and 'honest' way is to calculate three of the integrals (namely, over $\alpha, \beta, y$) via residues. That's what we are going to do.

The details of this calculations are given in Appendix A. Here we cite the result:

$$
\int dy \, dz \, d\alpha \, d\beta \, \frac{\Gamma}{[\text{all propagators}]}
$$
$$
= \left(-\frac{2\pi i}{s}\right)^3 \cdot \int \frac{dz}{z(1-z)} \psi_V(z, \vec{k}^2) \cdot \frac{1}{[\vec{k}_1^2 + m^2 + z(1-z)Q^2]} \frac{1}{(\vec{\kappa}^2 + \mu^2)^2} \tag{66}
$$

Here $\vec{k}_1$ is the transverse momentum flowing through photon vertex along the fermion line. Particularly, for diagr.(c) it is equal to $\vec{k}_1 = \vec{k} - (1-z)\vec{\Delta} - \vec{\kappa}_2$ (with the specific quark loop momentum choice given at Fig.(8a)).

Let us now stop for a moment and take a look at this result. As we know, aside from longitudinal momenta integration, we also have outer integrations over transverse gluon momenta $\int_0^\infty d^2\vec{\kappa}$. It will also be shown later that the upper loop will always (except for double spin flip amplitude) give factor $\vec{\kappa}^2$ in numerator. Thus, we will deal with integral

$$
\int_0^\infty d^2\vec{\kappa} \frac{\vec{\kappa}^2}{(\vec{\kappa}^2 + \mu^2)^2} \frac{1}{[(\vec{\kappa} - \vec{k} + (1-z)\vec{\Delta})^2 + m^2 + z(1-z)Q^2]} \,. \tag{67}
$$

This integral is naturally split up into three regions: $\vec{\kappa}^2 < \mu^2$, $\overline{Q}^2 > \vec{\kappa}^2 > \mu^2$, and $\vec{\kappa}^2 > \overline{Q}^2$. (Here we marked all low energy scales, namely, $\mu^2, m^2, \vec{\Delta}^2$ by a general parameter $\mu^2$.) A crucial observation here is that the largest contribution comes from the *perturbative* intermediate region

$$
\mu^2 \ll \vec{\kappa}^2 \ll \overline{Q}^2 \tag{68}
$$

due to an *extra large logarithmic factor* $\log(\overline{Q}^2/\mu^2)$ (which of course implies $\overline{Q}^2 \gg \mu^2$). **It is precisely the presence of this large logarithm that justifies our perturbative QCD approach**. Thus, we now established that in our problem the pQCD approach is valid only in the **leading log approximation** and has only logarithmic accuracy.

Thus, the amplitude for diagr.(c) has the form

$$
A = \sqrt{4\pi\alpha_{em}} \, 4 C_F N_c s^2 \, c_V \cdot \frac{1}{2} s \, \frac{1}{2} s \cdot \left(-\frac{2\pi i}{s}\right)^3 \cdot \frac{1}{(2\pi)^8}
$$
$$
\cdot \int \frac{dz}{z(1-z)} d^2\vec{k} \psi_V(z, \vec{k}^2) \int \frac{d^2\vec{\kappa} V(\kappa)}{(\vec{\kappa}^2 + \mu^2)^2} (4\pi\alpha_s)^2 \cdot \frac{I^{(c)}}{[\vec{k}_1^2 + m^2 + z(1-z)Q^2]} \,. \tag{69}
$$

After bringing all coefficients together, one gets

$$A^{(a)} = is \frac{C_F N_c c_V \sqrt{4\pi\alpha_{em}}}{(2\pi)^5} \cdot \int \frac{dz}{z(1-z)} d^2\vec{k}\psi_V(z,\vec{k}^2) \int \frac{d^2\vec{\kappa}V(\kappa)}{(\vec{\kappa}^2+\mu^2)^2}(4\pi\alpha_s)^2$$
$$\cdot \frac{I^{(c)}}{\vec{k}_1^2 + m^2 + z(1-z)Q^2} \cdot \tag{70}$$

The other diagrams are calculated in the same way. The most important difference is that for each diagram we will have a propagator $1/[\vec{k}_1^2 + m^2 + z(1-z)Q^2]$ with its own definition of $\vec{k}_1$, the transverse momentum in photon vertex:

$$\text{diagr.a} \quad \vec{k}_{1a} = \vec{k} - (1-z)\vec{\Delta} = \vec{r} - \frac{1}{2}\vec{\Delta}$$

$$\text{diagr.b} \quad \vec{k}_{1b} = \vec{k} - (1-z)\vec{\Delta} + \vec{\kappa} + \frac{1}{2}\vec{\Delta} = \vec{r} + \vec{\kappa}$$

$$\text{diagr.c} \quad \vec{k}_{1c} = \vec{k} - (1-z)\vec{\Delta} - \vec{\kappa} + \frac{1}{2}\vec{\Delta} = \vec{r} - \vec{\kappa}$$

$$\text{diagr.d} \quad \vec{k}_{1d} = \vec{k} + z\vec{\Delta} = \vec{r} + \frac{1}{2}\vec{\Delta} \tag{71}$$

Here $\vec{r} \equiv \vec{k} - (1-2z)\vec{\Delta}/2$. Thus, the whole expression for the imaginary part of the amplitude is

$$\begin{aligned}
A &= is\frac{C_F N_c c_V \sqrt{4\pi\alpha_{em}}}{(2\pi)^5} \cdot \int \frac{dz}{z(1-z)} d^2\vec{k}\psi_V(z,\vec{k}^2) \int \frac{d^2\vec{\kappa}V(\kappa)}{(\vec{\kappa}^2+\mu^2)^2}(4\pi\alpha_s)^2 \\
&\times \left[\frac{1-z}{z}\frac{I^{(a)}}{\vec{k}_{1a}^2 + m^2 + z(1-z)Q^2} + \frac{I^{(b)}}{\vec{k}_{1b}^2 + m^2 + z(1-z)Q^2}\right. \\
&\left.+ \frac{I^{(c)}}{\vec{k}_{1c}^2 + m^2 + z(1-z)Q^2} + \frac{z}{1-z}\frac{I^{(d)}}{\vec{k}_{1d}^2 + m^2 + z(1-z)Q^2}\right]. \tag{72}
\end{aligned}$$

## 3.7 Final exact results for the naive vertex

The only thing left to be computed is integrands $I^i(\gamma \to V)$. For convenience, their calculation is also given in Appendix B. It turns out that the results can be written in the same way for all four diagrams via $\vec{k}_1$ given by (71), i.e. all quantities:

$$-\frac{1-z}{z}I^{(a)}, \quad I^{(b)}, \quad I^{(c)}, \quad -\frac{z}{1-z}I^{(d)}$$

can be written in a similar way:

$$\begin{aligned}
T &\to T \quad \left[(\vec{e}\vec{V}^*)(m^2 + \vec{k}\vec{k}_1) + (\vec{V}^*\vec{k})(\vec{e}\vec{k}_1)(1-2z)^2 - (\vec{e}\vec{k})(\vec{V}^*\vec{k}_1)\right] \\
L &\to L \quad -4z^2(1-z)^2QM \\
T &\to L \quad 2z(1-z)M(\vec{e}\vec{k}_1)(1-2z) \\
L &\to T \quad -2z(1-z)Q(1-2z)(\vec{V}^*\vec{k})
\end{aligned}$$

Therefore, we can cast amplitude (72) in a compact form with aid of functions $\vec{\Phi}_1$ and $\Phi_2$:

$$\Phi_2 = -\frac{1}{(\vec{r}+\vec{\kappa})^2 + \overline{Q}^2} - \frac{1}{(\vec{r}-\vec{\kappa})^2 + \overline{Q}^2} + \frac{1}{(\vec{r}+\vec{\Delta}/2)^2 + \overline{Q}^2} + \frac{1}{(\vec{r}-\vec{\Delta}/2)^2 + \overline{Q}^2} \tag{73}$$

and

$$\vec{\Phi}_1 = -\frac{\vec{r}+\vec{\kappa}}{(\vec{r}+\vec{\kappa})^2+\overline{Q}^2} - \frac{\vec{r}-\vec{\kappa}}{(\vec{r}-\vec{\kappa})^2+\overline{Q}^2} + \frac{\vec{r}+\vec{\Delta}/2}{(\vec{r}+\vec{\Delta}/2)^2+\overline{Q}^2} + \frac{\vec{r}-\vec{\Delta}/2}{(\vec{r}-\vec{\Delta}/2)^2+\overline{Q}^2} \tag{74}$$

With these functions, for the naive $q\bar{q}V$ vertex the whole expression in square brackets in (72) wit sign minus (which we denote here as $I_{\lambda_\gamma \lambda_V}$) has the form:

$$\begin{aligned}
I_{LL} &= -4QMz^2(1-z)^2\Phi_2\,; \\
I_{TT} &= (\vec{e}\vec{V}^*)[m^2\Phi_2 + (\vec{k}\vec{\Phi}_1)] + (1-2z)^2(\vec{k}\vec{V}^*)(\vec{e}\vec{\Phi}_1) - (\vec{e}\vec{k})(\vec{V}^*\vec{\Phi}_1)\,; \\
I_{TL} &= 2Mz(1-z)(1-2z)(\vec{e}\vec{\Phi}_1)\,; \\
I_{LT} &= -2Qz(1-z)(1-2z)(V\vec{k})\Phi_2\,.
\end{aligned} \tag{75}$$

## 3.8 Gluon density

We have just calculated our reaction in the Born approximation. We understand however that the nature of $t$-channel exchange in diffractive processes is much more complicated. A physically meaningful procedure is to related this and other diffractive processes to the experimentally measurable gluon density. Here we explain a prescription of how to introduce unintegrated gluon density in answers calculated in the Born approximation.

A well known QED formula for Weizsaker-Williams approximations unambiguously defines the number of photons in an electron (in the Born approximation and to the logarithmic accuracy)

$$dn_\gamma = \frac{\alpha_{em}}{2\pi}[1+(1-\beta)^2]\frac{d\vec{\kappa}^2}{\vec{\kappa}^2}\frac{d\beta}{\beta} \approx \frac{\alpha_{em}}{\pi}\frac{d\vec{\kappa}^2}{\vec{\kappa}^2}\frac{d\beta}{\beta}\,. \tag{76}$$

Here $\beta$ is the fraction of electron energy carried by photon. Quantity

$$\rho_\gamma = \beta\frac{dn_\gamma}{d\beta} = \frac{\alpha_{em}}{\pi}\frac{d\vec{\kappa}^2}{\vec{\kappa}^2} \tag{77}$$

is called photon $\beta$-density. Thus, the unintegrated photon density is given by

$$\mathcal{F}^{(Born)} = \frac{\partial\rho_\gamma}{\partial\log\vec{\kappa}^2} = \frac{\alpha_{em}}{\pi}\,. \tag{78}$$

In QCD, in the Born approximation, one can define a similar quantity, namely, the unintegrated gluon density in a proton, which after careful accounting for all color factors reads:

$$\mathcal{F}^{(Born)} = \frac{\partial G}{\partial\log\vec{\kappa}^2} = C_F N_c \frac{\alpha_s}{\pi} V(\kappa)\,. \tag{79}$$

Therefore, a prescription of how to include unintegrated gluon density is as follows:

$$4\frac{\alpha_s}{\pi}V(\kappa) \equiv \mathcal{F}^{(Born)} \to \mathcal{F} \tag{80}$$

Finally, one has now to account for skewedness of this gluon density. Within diffraction cone (i.e. for $\vec{\Delta}^2$ up to several GeV$^2$) it is usually parameterized as

$$\mathcal{F}(x,\vec{\kappa},\vec{\Delta}) = \frac{\partial G(x,\vec{\kappa}^2)}{\partial\log\vec{\kappa}^2}\exp(-\frac{1}{2}B_{3\mathbb{P}}\vec{\Delta}^2)\,. \tag{81}$$

where $B_{3\mathbb{P}} \sim 6$ GeV$^{-2}$ is the so-called diffraction cone slope.

Therefore, a general amplitude of transition $\gamma^*_{\lambda_\gamma} \to V_{\lambda_V}$ has the following form

$$A(x, Q^2, \vec{\Delta}) = -is\frac{c_V\sqrt{4\pi\alpha_{em}}}{2\pi^2}\int_0^1 \frac{dz}{z(1-z)}\int d^2\vec{k}\psi(z,\vec{k})$$
$$\int \frac{d^2\vec{\kappa}}{\vec{\kappa}^4}\alpha_S\mathcal{F}(x, \vec{\kappa}, \vec{\Delta})\cdot I(\gamma^* \to V)\,, \tag{82}$$

## 3.9   Final results for $S$ and $D$ wave amplitudes

Now we can use projector technique to obtain results for $S/D$ wave states.

$$V_\mu \to V_\nu \mathcal{S}_{\nu\mu}\,;\quad \mathcal{S}_{\mu\nu} = g_{\mu\nu} - \frac{2p_\mu p_\nu}{m(M+2m)} \;\Rightarrow\; I^S = I + \frac{2(\mathbf{Vp})}{m(M+2m)}p_\mu \otimes \gamma_\mu\,; \tag{83}$$

$$V_\mu \to V_\nu \mathcal{D}_{\nu\mu}\,;\quad \mathcal{D}_{\mu\nu} = \mathbf{p}^2 g_{\mu\nu} + \frac{(M+m)p_\mu p_\nu}{m} \;\Rightarrow\; I^D = I\mathbf{p}^2 - \frac{(M+m)(\mathbf{Vp})}{m}p_\mu \otimes \gamma_\mu\,;$$

Note that $(\mathbf{Vp})$ is 3D scalar product. While contracting, we encounter terms proportional to $p_\mu \otimes \gamma_\mu$ which should be understood as

$$p_\mu \otimes \gamma_\mu = I_{V_T}\{\vec{V} \to \vec{p}\} + I_{V_L}\{1 \equiv V_z \to p_z \equiv \frac{1}{2}(2z-1)M\}. \tag{84}$$

The result of this substitution reads:
for $e_T$:

$$I_{T\to T}\{\vec{V} \to \vec{p}\} + I_{T\to L}\{1 \equiv V_z \to p_z \equiv \frac{1}{2}(2z-1)M\}$$
$$= m^2\left[(\vec{e}\vec{k})\Phi_2 - (\vec{e}\vec{\Phi}_1)(1-2z)^2\right] \tag{85}$$

for $e_0$:

$$I_{L\to T}\{\vec{V} \to \vec{p}\} + I_{L\to L}\{1 \equiv V_z \to p_z \equiv \frac{1}{2}(2z-1)M\}$$
$$= -2Qz(1-z)(2z-1)m^2\Phi_2 \tag{86}$$

So, the resulting integrands for $S$ wave type mesons are

$$I^S_{L\to L} = -4QMz^2(1-z)^2\left[1 + \frac{(1-2z)^2}{4z(1-z)}\frac{2m}{M+2m}\right]\Phi_2\,;$$

$$I^S_{T\to T} = (\vec{e}\vec{V}^*)[m^2\Phi_2 + (\vec{k}\vec{\Phi}_1)] + (1-2z)^2(\vec{k}\vec{V}^*)(\vec{e}\vec{\Phi}_1)\frac{M}{M+2m}$$
$$\qquad -(\vec{e}\vec{k})(\vec{V}^*\vec{\Phi}_1) + \frac{2m}{M+2m}(\vec{k}\vec{e})(\vec{k}\vec{V}^*)\Phi_2\,;$$

$$I^S_{T\to L} = 2Mz(1-z)(1-2z)(\vec{e}\vec{\Phi}_1)\left[1 + \frac{(1-2z)^2}{4z(1-z)}\frac{2m}{M+2m}\right] - \frac{Mm}{M+2m}(1-2z)(\vec{e}\vec{k})\Phi_2\,;$$

$$I^S_{L\to T} = -2Qz(1-z)(1-2z)(\vec{V}^*\vec{k})\frac{M}{M+2m}\Phi_2\,. \tag{87}$$

and for $D$ wave type mesons are

$$
\begin{aligned}
I^D_{L\to L} &= -QMz(1-z)\left(\vec{k}^2 - \frac{4m}{M}p_z^2\right)\Phi_2\,; \\
I^D_{T\to T} &= (\vec{e}\vec{V}^*)\mathbf{p^2}[m^2\Phi_2 + (\vec{k}\vec{\Phi}_1)] + (1-2z)^2(\mathbf{p}^2 + m^2 + Mm)(\vec{k}\vec{V}^*)(\vec{e}\vec{\Phi}_1) \\
&\quad -\mathbf{p}^2(\vec{e}\vec{k})(\vec{V}^*\vec{\Phi}_1) - m(M+m)(\vec{k}\vec{e})(\vec{k}\vec{V}^*)\Phi_2\,; \\
I^D_{T\to L} &= \frac{1}{2}M(1-2z)\left[(\vec{e}\vec{\Phi}_1)\left(\vec{k}^2 - \frac{4m}{M}p_z^2\right) + m(M+m)(\vec{e}\vec{k})\Phi_2\right]\,; \\
I^D_{L\to T} &= -2Qz(1-z)(1-2z)(\vec{V}^*\vec{k})(\mathbf{p}^2 + m^2 + Mm)\Phi_2\,.
\end{aligned}
\tag{88}
$$

Equations (87), (88) together with expression (82) constitute the ultimate sets of all helicity amplitudes. They give explicit answers for the vector meson production amplitudes within leading-log-approximation.

# 4 Analysis for heavy quarkonia

The general answers (87), (88) are of course incomprehensible at a quick glance. Therefore, a further analysis is needed to grasp the most vivid features of the results and to disentangle $s$-channel helicity conserving and double helicity flip amplitudes.

Since in the heavy vector mesons quarks can be treated non-relativistically, further simplifications in analytical formulas (87), (88) are possible due to the presence of an additional small parameter $\mathbf{p}^2/m^2$.

In what follows we will first perform the twist expansion and then relate simplified amplitudes to the decay constants (40), (41). We will then analyze twist hierarchy of the amplitudes and compare results for $S$ vs. $D$ wave states. Though we perform this analysis for heavy mesons, we wish to stress that all qualitative features ($S$ vs. $D$ difference, $Q^2$ dependence etc.) will hold for light quarkonia as well.

## 4.1 Twist expansion

Here we are going to expand the amplitudes (or to be more exact, the quantities $\vec{\Phi}_1$ and $\Phi_2$ (73), (74)) in inverse powers of the hard scale $\overline{Q}^2$ and then perform azimuthal angular averaging over $\phi_\kappa$.

Expanding $\Phi_2$ in twists in the main logarithmic region

$$\mu^2, \vec{\Delta}^2, \vec{k}^2 \ll \vec{\kappa}^2 \ll \overline{Q}^2 \,, \tag{89}$$

one observes that twist–1 terms cancel, so one has to retain twist–2 and twist–3 terms proportional $\vec{\kappa}^2$:

$$\Phi_2 = \frac{2\vec{\kappa}^2}{\overline{Q}^4} - \frac{8\vec{\kappa}^2\vec{r}^2}{\overline{Q}^6} \tag{90}$$

The analogous decomposition for $\vec{\Phi}_1$ reads

$$\vec{\Phi}_1 = \frac{4\vec{r}\vec{\kappa}^2}{\overline{Q}^4} - \frac{12\vec{r}\vec{\kappa}^2 r^2}{\overline{Q}^6} - \frac{\vec{\Delta}(\vec{r}\vec{\Delta})}{\overline{Q}^4} \tag{91}$$

Note that the last term does not contain $\vec{\kappa}^2$. However, one must track it because it will be important in double helicity flip amplitudes.

## 4.2 Twist expansion for $S$ wave type mesons

With the aid of this decomposition one obtains:
for amplitude $L \to L$

$$I_{L \to L}^S = -4QMz^2(1-z)^2\frac{2\vec{\kappa}^2}{\overline{Q}^4}\left[1 + \frac{(1-2z)^2}{4z(1-z)}\frac{2m}{M+2m}\right], \tag{92}$$

for amplitude $T \to T$

$$I_{T \to T}^S = (\vec{e}\vec{V}^*)\left[m^2\frac{2\vec{\kappa}^2}{\overline{Q}^4} + \frac{4\vec{\kappa}^2}{\overline{Q}^4}\vec{k}^2\right] + \frac{2m}{M+2m}\cdot\frac{1}{2}\vec{k}^2(\vec{e}\vec{V}^*)\frac{2\vec{\kappa}^2}{\overline{Q}^4} \tag{93}$$

$$+ \left[(1-2z)^2\frac{M}{M+2m} - 1\right]\left[\vec{k}^2(\vec{e}\vec{V}^*)\frac{2\vec{\kappa}^2}{\overline{Q}^4} - \frac{\vec{k}^2}{2\overline{Q}^4}(\vec{e}\vec{\Delta})(\vec{V}^*\vec{\Delta})\left(1 + \frac{6\vec{\kappa}^2(1-2z)^2}{\overline{Q}^2}\right)\right]$$

30

This amplitude is naturally split into $s$–channel helicity conserving and double helicity flip parts

$$
I^S_{T \to T}(\lambda_\gamma = \lambda_V) = (\vec{e}\vec{V}^*)\frac{2\vec{\kappa}^2}{\overline{Q}^4}\left[m^2 + 2\vec{k}^2(z^2 + (1-z)^2) + \frac{m}{M+2m}\vec{k}^2(1 - 2(1-2z)^2)\right]
$$

$$
I^S_{T \to T}(\lambda_\gamma = -\lambda_V) = 4z(1-z)(\vec{e}\vec{\Delta})(\vec{V}^*\vec{\Delta})\frac{\vec{k}^2}{2\overline{Q}^4}\left(1 + \frac{6\vec{\kappa}^2(1-2z)^2}{\overline{Q}^2}\right)\left[1 + \frac{(1-2z)^2}{4z(1-z)}\frac{2m}{M+2m}\right]
$$

$$(94)$$

Finally, single spin flip amplitudes are

$$
I^S_{T \to L} = -2Mz(1-z)(1-2z)^2\frac{2\vec{\kappa}^2}{\overline{Q}^4}(\vec{e}\vec{\Delta})\left[1 + \frac{(1-2z)^2}{4z(1-z)}\frac{2m}{M+2m}\right],
$$

$$
I^S_{L \to T} = -2Qz(1-z)(1-2z)^2\frac{2\vec{\kappa}^2}{\overline{Q}^4}(\vec{V}^*\vec{\Delta})\frac{2\vec{k}^2}{\overline{Q}^2}\frac{M}{M+2m}.
$$

$$(95)$$

## 4.3   Twist expansion for $D$–type vector mesons

Here we will need to track higher–twist terms. It will turn out later that leading contributions vanish, so twist–3 terms will be crucial for our results.
For amplitude $L \to L$ one has

$$
I^D_{L \to L} = -QMz(1-z)\left(\vec{k}^2 - \frac{4m}{M}p_z^2\right) \cdot \frac{2\vec{\kappa}^2}{\overline{Q}^4}\left(1 - \frac{4\vec{k}^2}{\overline{Q}^2}\right).
$$

$$(96)$$

For $T \to T$ amplitude, one obtains

$$
I^D_{T \to T} = (\vec{e}\vec{V}^*)\mathbf{p}^2\left[m^2\frac{2\vec{\kappa}^2}{\overline{Q}^4}\left(1 - \frac{4\vec{k}^2}{\overline{Q}^2}\right) + \frac{2\vec{\kappa}^2}{\overline{Q}^4}2\vec{k}^2\right]
$$

$$
+ \left[-4z(1-z)\mathbf{p}^2 + (1-2z)^2m(M+m)\right]\left\{\frac{2\vec{\kappa}^2}{\overline{Q}^4}\vec{k}^2(\vec{e}\vec{V}^*) - \frac{\vec{k}^2}{2\overline{Q}^4}(\vec{e}\vec{\Delta})(\vec{V}^*\vec{\Delta})\left[1 + \frac{6\vec{\kappa}^2(1-2z)^2}{\overline{Q}^2}\right]\right\}
$$

$$
-m(M+m)\frac{1}{2}\vec{k}^2(\vec{e}\vec{V}^*)\frac{2\vec{\kappa}^2}{\overline{Q}^4}\left(1 - \frac{4\vec{k}^2}{\overline{Q}^2}\right)
$$

$$(97)$$

Note that we kept track of all terms $\propto |p|^4$. Again, one can separate out $s$-channel helicity conserving and double helicity flip parts:

$$
I^D_{T \to T}(\lambda_\gamma = \lambda_V) = (\vec{e}\vec{V}^*)\frac{\vec{\kappa}^2}{\overline{Q}^4}\left[2\mathbf{p}^2\left(m^2 + 2\vec{k}^2 - 4\vec{k}^2\frac{m^2}{\overline{Q}^2}\right) - m(M+m)\vec{k}^2\left(1 - \frac{4\vec{k}^2}{\overline{Q}^2}\right)\right.
$$

$$
\left. -2\vec{k}^2\left(\vec{k}^2 - \frac{4m}{M}p_z^2\right)\right]
$$

$$
I^D_{T \to T}(\lambda_\gamma = -\lambda_V) = \left(\vec{k}^2 - \frac{4m}{M}p_z^2\right)(\vec{e}\vec{\Delta})(\vec{V}^*\vec{\Delta})\frac{\vec{k}^2}{2\overline{Q}^4}\left(1 + \frac{6\vec{\kappa}^2(1-2z)^2}{\overline{Q}^2}\right)
$$

$$(98)$$

Finally, single helicity flipping amplitudes are

$$
\begin{aligned}
I^D_{T \to L} &= \frac{1}{2} M(1-2z) \left[ \frac{-2(1-2z)(\vec{e}\vec{\Delta})\vec{\kappa}^2}{\overline{Q}^4} \left( \vec{k}^2 - \frac{4m}{M} p_z^2 \right) + m(M+m) \frac{4\vec{\kappa}^2 \vec{k}^2}{\overline{Q}^6}(1-2z)(\vec{e}\vec{\Delta}) \right] \\
&= -\frac{\vec{\kappa}^2}{\overline{Q}^4}(1-2z)^2 M(\vec{e}\vec{\Delta}) \left[ \vec{k}^2 - \frac{4m}{M} p_z^2 - m(M+m) \frac{2\vec{k}^2}{\overline{Q}^2} \right], \\
I^D_{L \to T} &= -8Qz(1-z)(1-2z)^2(\mathbf{p}^2 + m^2 + mM) \frac{\vec{\kappa}^2}{\overline{Q}^6} \vec{k}^2 (\vec{V}^*\vec{\Delta}).
\end{aligned}
\tag{99}
$$

## 4.4 Final results for $S$ wave mesons

In order to grasp the major features of various $S$ and $D$ wave amplitudes, further simplifications can be achieved if one neglects spherically non-symmetric arguments of $\alpha_s$ and gluon density. First we rewrite general expression (82) in the more convenient form

$$
A(x, Q^2, \vec{\Delta}) = -is \frac{c_V \sqrt{4\pi\alpha_{em}}}{2\pi^2} \int d^3\mathbf{p} \frac{4}{M} \psi(\mathbf{p}^2) \int \frac{d^2\vec{\kappa}}{\kappa^4} \alpha_S \mathcal{F} \cdot I(\gamma^* \to V).
\tag{100}
$$

In this expression everything except for integrands $I(\gamma^* \to V)$ is spherically symmetric, thus making it possible to perform angular averaging over $\Omega_{\mathbf{p}}$ in these integrands.

### 4.4.1 $S$ wave: $\Omega_{\mathbf{p}}$ averaging

Here all the calculations are rather straightforward. In the non-relativistic case one can everywhere put $z \to 1/2$; $M = 2m = m_V$. The resultant integrands are:

$$
\begin{aligned}
I^S(L \to L) &= -\frac{8QM}{(Q^2+M^2)^2} \vec{\kappa}^2 \\[2mm]
I^S(T \to T; \lambda_\gamma = \lambda_V) &= \frac{8M^2}{(Q^2+M^2)^2} \vec{\kappa}^2 \\[2mm]
I^S(T \to T; \lambda_\gamma = -\lambda_V) &= \frac{16}{3} \frac{(\vec{e}\vec{\Delta})(\vec{V}^*\vec{\Delta})}{(Q^2+M^2)^2} \left[ 1 + \frac{96}{5} \frac{\vec{\kappa}^2 \mathbf{p}^2}{M^2(Q^2+M^2)} \right] \\[2mm]
I^S(T \to L) &= -\frac{64}{3} \frac{M(\vec{e}\vec{\Delta})}{(Q^2+M^2)^2} \frac{\mathbf{p}^2}{M^2} \vec{\kappa}^2 \\[2mm]
I^S(L \to T) &= -\frac{512}{15} \frac{Q(\vec{V}^*\vec{\Delta})}{(Q^2+M^2)^2} \frac{\mathbf{p}^4}{M^2(Q^2+M^2)} \vec{\kappa}^2
\end{aligned}
\tag{101}
$$

Note several things: since the accurate $1S$ wave differs from the naive $\gamma_\mu$ spinorial structure only by relativistic corrections, one would obtain *the same results* in the case of naive $q\bar{q}V$ vertex. The only difference would be only extra factor 2 for the $L \to T$ amplitude (which is higher-twist amplitude, anyway).

Thus the only thing left is $|\mathbf{p}|$ integration. Note that these amplitudes are naturally expressed in terms of decay constants. Indeed, in the extremely non-relativistic case expression (40) turns into

$$f^{(S)} = \frac{3m_V}{2\pi^3}\int d^3\mathbf{p}\,\psi_S \quad \Rightarrow \quad \int d^3\mathbf{p}\,\psi_S = \frac{2\pi^3}{3m_V}f^{(S)} \tag{102}$$

### 4.4.2   $S$ wave: answers for $L \to L$ up to differential cross section

Here we would like to digress and for the sake of logical completeness show how one obtains the final result for the differential cross section with the example of $L \to L$ amplitude. If needed, the same can be done for the other amplitudes, so we will do it just once.

One has:

$$\int d^3\mathbf{p}\,\psi_S\frac{4}{m_V}\frac{-8Qm_V}{(Q^2+m_V^2)^2}\cdot\pi\int^{\overline{Q}^2}_{\overline{Q}^2}\frac{d\vec{\kappa}^2}{\vec{\kappa}^2}\frac{\partial G(x,\vec{\kappa}^2)}{\partial\log\vec{\kappa}^2}\alpha_s(\vec{\kappa}^2)\exp(-\frac{1}{2}B_{3\mathbf{P}}\vec{\Delta}^2)$$

$$= -\frac{32\pi Q}{(Q^2+m_V^2)^2}G(x,\overline{Q}_0^2)\alpha_s(\overline{Q}_0^2)\exp(-\frac{1}{2}B_{3\mathbf{P}}\vec{\Delta}^2)\int d^3\mathbf{p}\,\psi_S$$

$$= -\frac{32\pi Q}{(Q^2+m_V^2)^2}\exp(-\frac{1}{2}B_{3\mathbf{P}}\vec{\Delta}^2)G(x,\overline{Q}_0^2)\alpha_s(\overline{Q}_0^2)\frac{2\pi^3}{3m_V}f_V$$

With this result, (100) becomes

$$A = is\frac{f_Vc_V\sqrt{4\pi\alpha_{em}}}{2\pi^2}\cdot\frac{64\pi^4}{3}\frac{Q}{m_V}\frac{G\cdot\alpha_s}{(Q^2+m_V^2)^2}$$

$$= is\frac{32\pi^2}{3}\frac{Q}{m_V}\cdot c_Vf_V\cdot\sqrt{4\pi\alpha_{em}}\frac{G\cdot\alpha_s\exp(-\frac{1}{2}B_{3\mathbf{P}}\vec{\Delta}^2)}{(Q^2+m_V^2)^2}$$

The expression for the differential cross section reads ($t \equiv \vec{\Delta}^2$):

$$\frac{d\sigma}{dt} = \frac{1}{16\pi s^2}|A|^2$$

$$= \frac{64\pi^3}{9}\frac{Q^2}{m_V^2}\cdot(c_Vf_V)^24\pi\alpha_{em}\cdot\frac{G^2\alpha_s^2\exp(-B_{3\mathbf{P}}t)}{(Q^2+m_V^2)^4}\,.$$

Finally, one can express this cross section through $\Gamma(V \to e^+e^-)$ (see (42)):

$$\boxed{\frac{d\sigma}{dt} = \frac{64\pi^3}{3\alpha_{em}}Q^2m_V\cdot\Gamma(V \to e^+e^-)\cdot\frac{G^2\alpha_s^2\exp(-B_{3\mathbf{P}}t)}{(Q^2+m_V^2)^4}\,.} \tag{103}$$

### 4.4.3   $S$ wave: the other amplitudes

$T \to T, \lambda_\gamma = \lambda_V$.
In the non-relativistic case, this amplitude is readily obtained from the above formulas after $Q \to m_V$ replacement in the numerator of the amplitude (see (101)). This means in particular that in this limit

$$R^{(S)} \equiv \left(\frac{A_{LL}}{A_{TT}}\right)^2 = \frac{Q^2}{m_V^2}\,. \tag{104}$$

$T \to T, \lambda_\gamma = -\lambda_V$.

This amplitude is very interesting because of the competition of two very different terms — soft and hard scale contribution. Indeed, integration over gluon loop gives

$$A \propto \frac{G(x, \mu^2)}{\mu^2} + \frac{96}{5} \frac{G(x, \overline{Q}^2)\mathbf{p}^2}{M^2(Q^2 + M^2)} \tag{105}$$

We see that the soft contribution turns out to be of leading twist, while the pQCD contribution is of higher twist. This observation was first made in [6] for the naive type of $q\bar{q}V$ vertex; here we see that it also holds for accurate $S$ and $D$ wave vector mesons.

Since at moderate $Q^2$ both terms can be comparable, we cannot neglect soft scale contribution, which means that we failed to compute the double helicity flip amplitude within pQCD approach.

$T \to L$ **and** $L \to T$.

In the case of heavy quarkonia these single spin flip amplitudes have suppressing non-relativistic factors. Besides, the amplitude $L \to T$ is of twist 3, which is another source of suppression. Their ratios to $A(T \to T) \equiv A(T \to T; \lambda_\gamma = \lambda_V^*)$ read

$$\frac{A(T \to L)}{A(T \to T)} = -\frac{8}{3} \frac{(\vec{e}\vec{\Delta})}{m_V} \cdot w_2; \quad \frac{A(L \to T)}{A(T \to T)} = -\frac{64}{15} \frac{Q(\vec{V}^*\vec{\Delta})}{Q^2 + m_V^2} \cdot w_4. \tag{106}$$

The model dependent quantities $w_2$ and $w_4$ are defined via

$$w_2 = \frac{1}{m_V^2} \frac{\int d^3\mathbf{p} \; \mathbf{p}^2 \; \psi_S}{\int d^3\mathbf{p} \; \psi_S}; \quad w_4 = \frac{1}{m_V^4} \frac{\int d^3\mathbf{p} \; \mathbf{p}^4 \; \psi_S}{\int d^3\mathbf{p} \; \psi_S}. \tag{107}$$

Within the oscillator ansatz (45) their values are

$$w_2 = \frac{3}{2} \frac{1}{(m_V R)^2}; \quad w_4 = \frac{15}{4} \frac{1}{(m_V R)^4}. \tag{108}$$

## 4.5   Final results for $D$ wave

This case is much more tricky. It turns out that the leading terms in integrands $I^{(D)}$, proportional to $m^2|p|^2$ cancel out after angular averaging, so that many new terms, including higher twist terms come into play. This cancellation is in fact quite understandable. Indeed, in the very beginning we showed that vertex $\bar{u}'\gamma_\mu u$ contains both $S$ and $D$ waves, with $D$ wave probability being suppressed for heavy quarks due to non-relativistic motion. This means in particular that the *photon* couples to $q\bar{q}$ pairs sitting either in $S$ or $D$ wave state. However, at the other end of the quark loop we have a vector meson in pure $D$ wave state. Therefore, the largest items in $\langle \gamma_{S+D}|...|V_D \rangle$ cancel out due to $S$–$D$ orthogonality.

### 4.5.1   $D$ wave: $\Omega_\mathbf{p}$ averaging for $L \to L$ amplitude

If we limited ourselves only to the leading $\mathbf{p}^2/m^2$ terms, we would get

$$\int d\Omega_\mathbf{p} \left( \vec{k}^2 - \frac{4m}{M} p_z^2 \right) = 4\pi \cdot \left( \frac{2}{3}\mathbf{p}^2 - 2 \cdot \frac{1}{3}\mathbf{p}^2 \right) = 0,$$

which is the manifestation of $S$–$D$ orthogonality. Thus, we see that $\mathbf{p}^2/m^2$ terms vanish after angular averaging. Therefore, one has to be extremely careful now and must take into account all possible sources of $\mathbf{p}^4/m^4$ terms. To do so, one has to perform the following averaging

$$\left\langle 4z(1-z) \cdot \frac{1}{\overline{Q}^4} \cdot \left( \vec{k}^2 - \frac{4m}{M}p_z^2 \right) \cdot \left( 1 - \frac{4\vec{k}^2}{\overline{Q}^2} \right) \right\rangle \tag{109}$$

The detailed evaluation given in Appendix C results in

$$\frac{1}{\overline{Q}_0^4} \frac{4\mathbf{p}^4}{15M^2} \left( 1 - 8\frac{M^2}{Q^2+M^2} \right) ,$$

where $\overline{Q}_0^2 = m^2 + Q^2/4$. One can now again express the integral over quark loop through the decay constant (see (41)):

$$\int d^3\mathbf{p} \; \mathbf{p}^4 \; \psi_D \Rightarrow f^{(D)} \cdot \frac{\pi^3 m_V}{2} . \tag{110}$$

to give

$$-\frac{64\pi^4}{15} \frac{Q}{m_V} \frac{G \cdot \alpha_s \cdot \exp(-\frac{1}{2}B_{3\mathbf{P}}\vec{\Delta}^2)}{(Q^2+m_V^2)^2} \cdot f^{(D)} \cdot \left( 1 - 8\frac{m_V^2}{Q^2+m_V^2} \right) \tag{111}$$

Comparison with $L \to L$ amplitude reveals that

$$\boxed{\frac{A_{LL}^D}{A_{LL}^S} = \frac{1}{5} \left( 1 - 8\frac{m_V^2}{Q^2+m_V^2} \right) \cdot \frac{f^{(D)}}{f^{(S)}} .}$$

$$\tag{112}$$

### 4.5.2   $D$ wave: the other amplitudes

For the helicity conserving amplitude one has to repeat the same averaging procedure, which is again fully elaborated in Appendix C. The result can be written as

$$\boxed{\frac{A_{LL}^D}{A_{TT}^D} = \frac{1}{15} \frac{1 - 8\dfrac{m_V^2}{Q^2+m_V^2}}{1 + \dfrac{4}{15}\dfrac{m_V^2}{Q^2+m_V^2}} .}$$

$$\tag{113}$$

In the case of double helicity flip amplitude we again have contributions from soft and hard scales with the same hierarchy of twists. Namely,

$$A \propto \frac{G(x,\mu^2)}{\mu^2} - \frac{96}{7} \frac{G(x,\overline{Q}^2)\mathbf{p}^2}{M^2(Q^2+M^2)} \tag{114}$$

so we again conclude that for the case of double helicity flip amplitude soft contribution invalidates our pQCD analysis.

In the case of single spin flip amplitudes, no dangerous calcellations among leading terms arise. Before giving a list of amplitudes, we wish to emphasize that in the case of $D$ wave mesons there is no non-relativistic suppressing factors like $w_2$ and $w_4$ defined in (107). This means that for moderate momentum transfers helicity non-conserving amplitudes are absolutely important for that case of $D$ wave mesons.

## 4.6   $S$ wave vs. $D$ wave comparison

We would like to present our final results in the form which stresses the remarkable differences between $S$ wave and $D$ wave amplitudes. Below we give a table of the ratios

$$\rho_{ij} \equiv \frac{A^D(i \to j)}{A^S(i \to j)} \frac{f^{(S)}}{f^{(D)}} \tag{115}$$

for helicity conserving and single spin flipping amplitudes. Double spin flip amplitudes are not given due to the presence of incalculable non-perturbative contributions.

$$
\begin{aligned}
\rho_{LL} &= \frac{1}{5}\left(1 - 8\frac{m_V^2}{Q^2 + m_V^2}\right) \\
\rho_{TT} &= 3\left(1 + \frac{4}{15}\frac{m_V^2}{Q^2 + m_V^2}\right) \\
\rho_{TL} &= -\frac{3}{5}\frac{1}{w_2}\left(1 + 3\frac{m_V^2}{Q^2 + m_V^2}\right) \\
\rho_{LT} &= \frac{9}{8}\frac{1}{w_4}
\end{aligned}
\tag{116}
$$

Thus, we note several things. First, the abnormally large higher twist contributions to $D$ wave amplitudes are seen here as terms $\propto m_V^2/(Q^2 + m_V^2)$. They even force the opposite sign of $L \to L$ amplitude in the moderate $Q^2$ domain. Second, we see highly non–trivial and even non–monotonous $Q^2$ dependence of $(A_{LL}/A_{TT})^2$ ratio, which will lead to the presence of a dip in experimentally measured $\sigma_L/\sigma_T$ for $D$ wave meson production. Finally, we must stress that in the case of $D$ wave mesons there is no non-relativistic suppression for single spin flip amplitudes as it was in $S$ wave mesons. This leads us to a conclusion that $s$-channel helicity is strongly violated in the case of $D$ wave meson production.

*Spin density matrix for diffractive* ρ *at HERA*
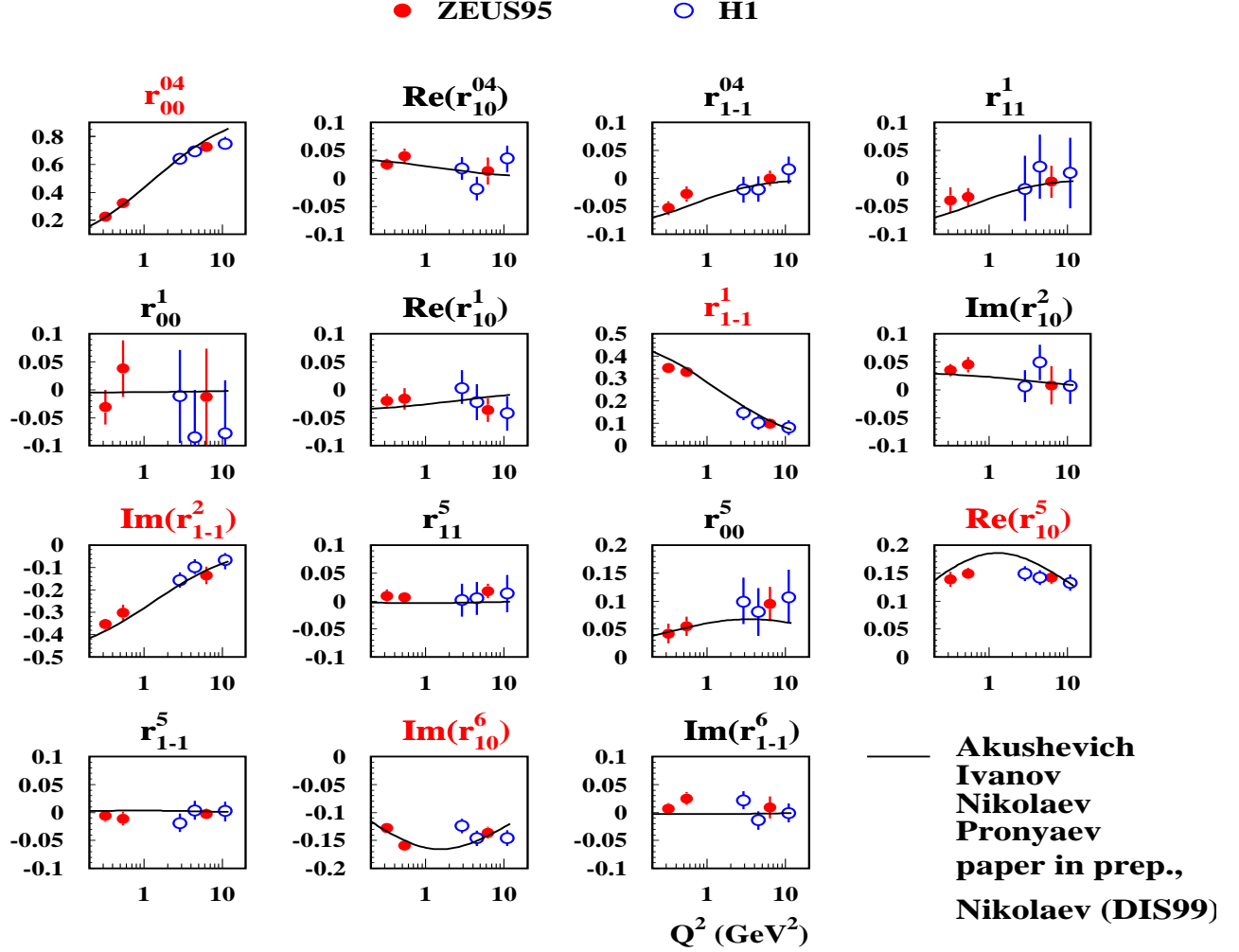
(Schilling-Wolf conventions)

Figure 10: The $\rho$ meson spin density matrix: comparison of recent HERA data with our predictions for $1S$ state.

# 5 Numerical analysis

In this section we will present some results of the numerical investigation. These results bear mostly illustrative purpose. Undoubtedly, they do not exhaust all interesting issues and leave much room for further numerical analysis.

Everywhere in our analysis we used oscillator type wave functions (45) with $R_D = R_{1S}$. There are several parameters to vary in order to achive the most correct description of the vector mesons. Aside from the very ansatz for the wave function, which is now fixed, we also have quark mass $m$ and radius $R$ as free parameters. We stress that these are purely
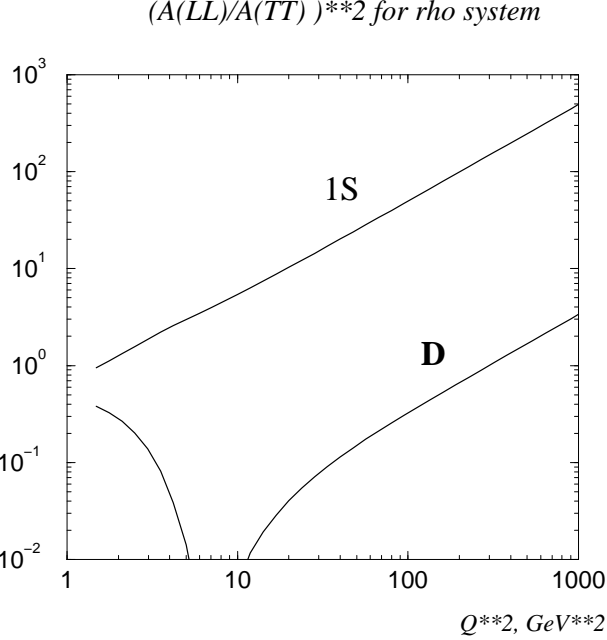
*(A(LL)/A(TT) )\*\*2 for rho system*

Figure 11: Ratio $[A(L \to L)/A(T \to T)]^2$ for $S$ and $D$ states in $\rho$ system at fixed $x = 0.01$ as a function of $Q^2$.

phenomenological parameters; in particular, it would be a mistake to assign values of several MeV to the quark masses. In principle, these quark masses can even vary from the ground to excited states for the same quarkonium.

We used normalization conditions (32) and (34) to determine normalization constants and chose a specific pair $m$, $R$ to have the decay constant coinciding with the experimental values. To avoid unnecessarily many free parameters, we used the same values for $S$ and $D$ wave states. Specifically, for the $\rho$ meson we took $m = 0.3$ GeV and $R = 4.0$ GeV$^{-1}$ (which corresponds 0.8 fm). For charmonium the value were $m = 1.3$ GeV and $R = 1.5$ GeV$^{-1} = 0.3$ fm.

Because all quantities displayed in figures are ratios of one amplitude to another, these results are not sensitive to the particular gluon distribution parameterization. Since we leave double helicity flip amplitudes aside, we can now switch to the integrated gluon density

$$ G(x, \overline{Q}^2) \exp(B_{3\mathbb{P}} \vec{\Delta}^2) = \int \frac{d\vec{\kappa}^2}{\vec{\kappa}^2} \mathcal{F} . $$

So, we used the integrated form of GRV parameterization with a linear extrapolation of gluon density in the region $Q^2 < 1$ GeV$^2$ so that $G(x, Q^2) \to 0$ when $Q^2 \to 0$. In fact, in an accurate numerical analysis low $Q^2$ region should be treated more carefully. Indeed, parton distributions do not evolve in this region, however, they can be parameterized with aid of low energy experimental data.

In Fig.10 we compare our calculations for $\rho$ vector meson density matrix with recent experimental data from HERA [20]. We see that our calculations describe data reasonable well, including parameters connected with $s$-channel helicity violation.

In Fig.11 we show ratio $(A_{LL}/A_{TT})^2$ (which would be $\sigma_L/\sigma_T$ if the $s$-channel helicity were

$$|A(TL)/A(TT)|$$

*rho system*

*Q\*\*2, GeV\*\*2*

*Charmonium*

*Q\*\*2, GeV\*\*2*
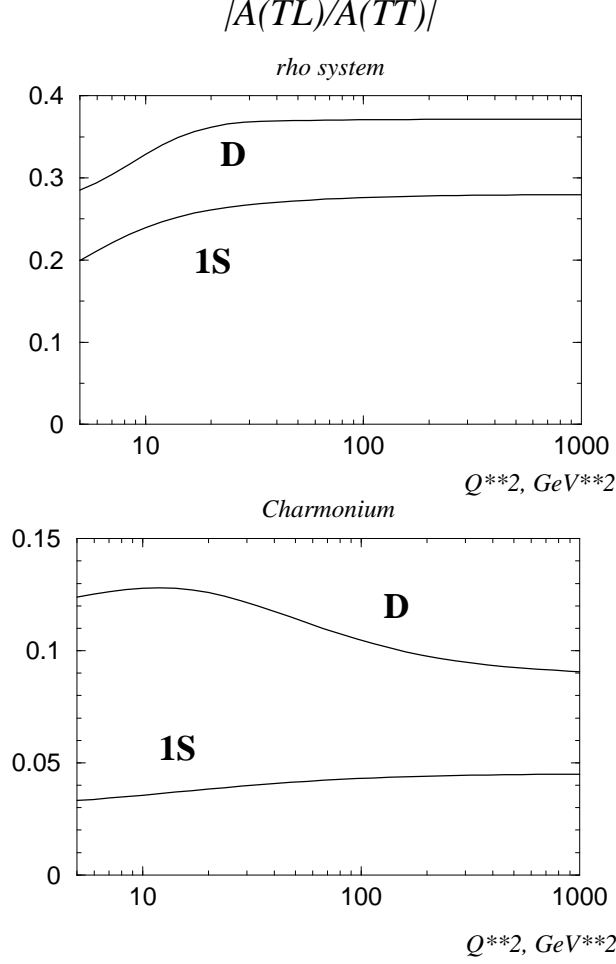
Figure 12: The absolute value of ratio $A(T \to L)/A(T \to T)$ revealing the relative magnitude of $T \to L$ spin flipping amplitude at fixed $x = 0.01$ as a function of $Q^2$. The sign of this ratio is $-$ for $S$ wave and $+$ for $D$ wave states.

conserved) for both $S$ and $D$ wave states of $\rho$ and $J/\psi$ system. A striking difference is observed both at small and large $Q^2$.

In Figs.12, 13 we present the relative magnitude of helicity non-conserving amplitudes again for $S$ and $D$ states in $\rho$ and $J/\psi$ system. It is interesting to note that $T \to L$ amplitudes have opposite signs for $S$ and $D$ wave mesons. We underline the large helicity violating amplitudes in $D$ wave states, both in non-relativistic $J/\psi$ and fully relativistic $\rho$ meson. The size of the effect reaches 35% for $\rho$ system and 13% for charmonium. Thus, it becomes now quite obvious that in the case of $D$ wave mesons no helicity conservation holds even at the qualitative level, in accordance with our previous conclusion from the heavy quarkonia analysis.

Finally, we analyzed the possibility of $S - D$ mixing in the physical $\rho$ meson. Namely, we introduced mixing angle $\theta$ as

$$\rho_{phys} = \cos\theta|1S\rangle + \sin\theta|D\rangle \tag{117}$$

and plotted ratio $(A_{LL}/A_{TT})^2$ in Fig.14 for mixing angles $\theta = \pm 20°$. The results are strikingly

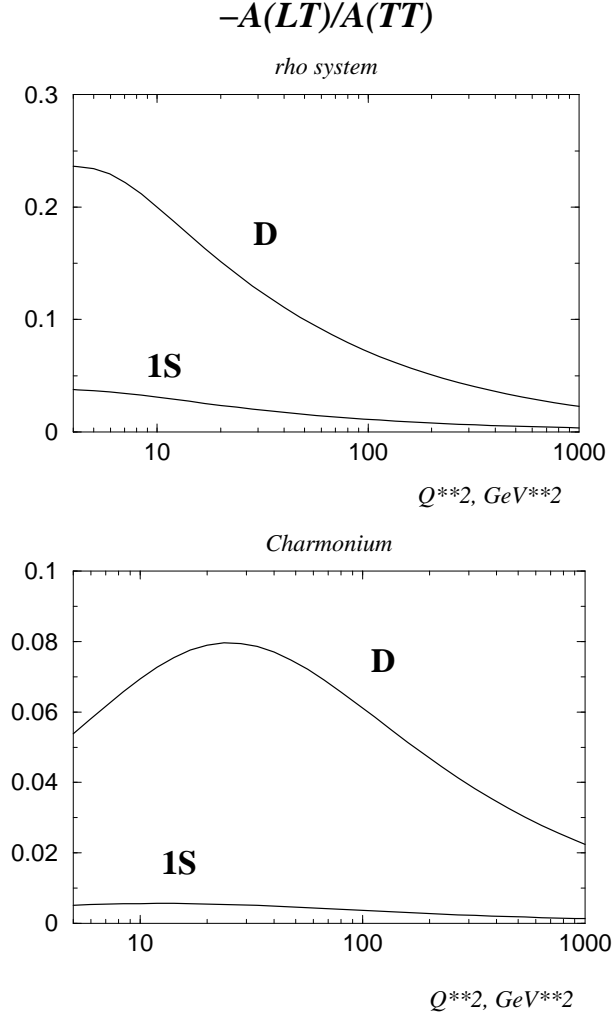**−A(LT)/A(TT)**

*rho system*

*Q\*\*2, GeV\*\*2*

*Charmonium*

*Q\*\*2, GeV\*\*2*

Figure 13: The ratio $-A(L \to T)/A(T \to T)$ showing the relative magnitude of $L \to T$ spin flipping amplitude at fixed $x = 0.01$ as a function of $Q^2$. It is seen that this transition is of higher twist.

sensitive to the presence of $D$ wave admixture in the physical $\rho$ meson; further investigation of this phenomenon is needed.
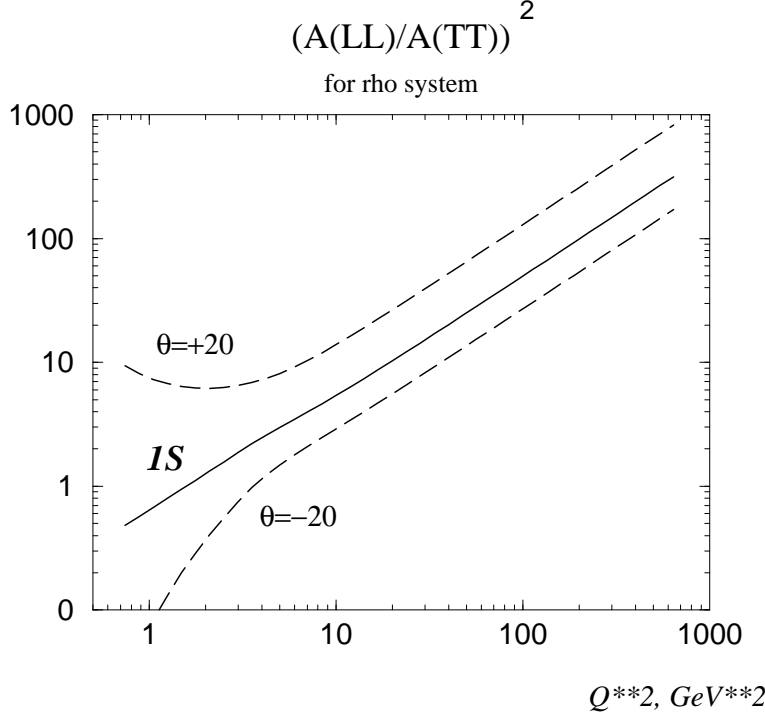
Figure 14: The impact of possible $S - D$ mixing in the physical $\rho$ meson on the ratio $[A(L \rightarrow L)/A(T \rightarrow T)]^2$ at fixed $x = 0.01$ as a function of $Q^2$.

# 6   Conclusion

In this work we brought under an accurate analysis the issue of internal vector meson spin structure in its diffractive production in DIS. In fact, we developed an essentially new way to study the internal spin structure of a vector meson.

To do so, we elaborated a formalism of treating pure $S$ and $D$ wave vector mesons in such processes. For the first time, the full sets of helicity amplitudes in both cases were calculated. The exact results (82), (87), (88) were derived within pQCD leading log approximation and then analyzed analytically in the limiting case of heavy vector mesons (103), (104), (106), (116) and numerically in the case of $\rho$ system and charmonium (Figs. 10–14).

In particular, for the $s$-channel helicity conserving amplitudes we observed:

- remarkably different $Q^2$-dependence of $S$ and $D$ wave type amplitudes, providing thus a way to discern $S$ and $D$ wave states that are indistinguishable at $e^+e^-$ colliders;

- dramatic role of higher twist contributions to the $D$ wave vector mesons, which even forced sign change for $L \rightarrow L$ amplitude and led to non-monotonous $\sigma_L/\sigma_T$ ratio;

- in the case of light vector mesons we found that $D$ wave amplitudes are absolutely comparable with $S$ wave, making, for example, the physical $\rho$ meson very sensitive to the possible presence of $D$ wave admixture.

Our results for helicity violating amplitudes include:

- observation that they are not negligible for light vector mesons of $S$ wave type, but become suppressed for heavy $S$ wave mesons;

41

- very large helicity violating effects for $D$ wave vector states, which do not get suppressed even in the case of heavy quarkonia;

- opposite signs for the largest spin flip amplitude $T \to L$ for $S$ and $D$ wave vector mesons;

- confirmation of the soft dominance of the double spin flip amplitude in the case of accurate $S$ and $D$ wave states.

Though we performed some numerical analysis, there is much room for further investigation. In particular, more extensive analysis is needed to check the model dependence of the numerical results obtained. It is also desirable to give definite numerical predictions for diffractive DIS experiments.

# References

[1] N.N. Nikolaev and B.G. Zakharov, "Phenomenology of Diffractive DIS", Talk given at 5th International Workshop on Deep Inelastic Scattering and QCD (DIS 97), Chicago, IL, 14-18 Apr 1997, **hep-ph/9706343**.

[2] A.C. Irving, R.P. Worden, *Phys.Rept.* **34** (1977) 117-231.

[3] V.S. Fadin, E.A. Kuraev, L.N. Lipatov, *Phys.Lett.* **B 60** (1975) 60; E.A. Kuraev, L.N. Lipatov, V.S. Fadin, *Sov. Phys. JETP* **44**, (1976) 443; **72** (1977) 377; Ya.Ya. Balitskii, L.N.Lipatov, *Sov.J.Nucl.Phys.* **28** (1978) 822.

[4] L.N. Lipatov and V.S. Fadin, *JETP Lett.* **49** (1995); L.N. Lipatov, *Phys.Rept.* **286** (1997) 131-198.

[5] *for an introductory text see* E. Levin, *Heavy Ion Phys.* **8**:265-283,1998, hep-ph/9808483; E. Levin, *"The Pomeron: yesterday, today and tomorrow"*, Lectures given at 3rd Gleb Wataghin School on High Energy Phenomenology, Campinas, Brazil, 11-16 Jul 1994, **hep-ph/9503399**

[6] D.Yu. Ivanov, R. Kirschner, *Phys.Rev.* **D58** (1998),114026.

[7] E.V.Kuraev, N.N.Nikolaev, and B.G.Zakharov, *JETF Lett.* 68(1998) 667.

[8] K. Schilling, G. Wolf, *Nucl.Phys.* **B 61**(1973) 381.

[9] N.N. Nikolaev, *Comments on Nucl.Part.Phys.* **21** (1992) 41; B.Z. Kopeliovich, J. Nemchik, N.N. Nikolaev and B.G. Zakharov, *Phys. Lett.* **B 309** (1993) 179; *Phys. Lett.* **B 324** (1994) 469.

[10] D.Yu. Ivanov, *Phys. Rev.* **D 53** (1996) 3564; I. Ginzburg, S. Panfil and V. Serbo, *Nucl. Phys.* **B 284** (1987) 685; **B 296** (1988) 569.

[11] J.Nemchik, N.N.Nikolaev and B.G.Zakharov, *Phys. Lett.* **B339** (1994) 194-200.

[12] D.O. Riska, *Acta Phys.Polon.* **B29** (1998) 2389.

[13] I.P.Ivanov, N.N.Nikolaev, *Pis'ma ZhETF (JETP Lett.)* **69** (1999) 268, hep-ph/9901267.

[14] I.P. Ivanov, *"Diffractive production of S and D wave vector mesons in DIS"*, talk given at *DPG Tagungen*, Heidelberg, 15-19 Mar. 1999.

[15] N.N. Nikolaev, *"Spin dependence in Diffractive DIS"*, talk given at *DIS 99*, Berlin, 18-24 Apr. 1999.

[16] M.V. Terentev, *Sov. J. Nucl. Phys.* **24** (1976) 106; **Yad. Fiz. 24** (1976) 207; V.B. Berestetskii and M.V. Terentev, **Yad. Fiz. 25** (1977) 653; L.A. Kondratyuk and M.V. Terentev, *Sov. J. Nucl. Phys.* **31** (1980) 561; **Yad. Fiz. 31** (1980) 1087.

[17] J. Bjorken, J. Kogut, D. Soper, *Phys. Rev.* **D 3**(1971) 1382; G.P. Lepage, S.J. Brodsky, *Phys. Rev.* **D 22**(1980) 2157; S. Brodsky, H.-Ch. Pauli, S. Pinsky, *Phys. Rept.* **301**, (1998), 299-486; T. Heinzl, **hep-th/9812190**, 1998.

[18] V.V. Sudakov, *Sov.Phys.JETP* 3:65-71,1956, *Zh.Eksp.Teor.Fiz.*30:87-95,1956.

[19] V.V. Anisovich *et al.*, *Nucl. Phys.* **A 563** (1993) 549–583; W. Jaus, *Phys. Rev.* **D 41**(1990) 3394; *Phys. Rev.* **D 44**(1990) 2851.

[20] H1 coll. *"Elastic electroproduction of rho mesons at HERA"*, **hep-ex/9902019**; P. Marage, **hep-ph/9904255**.

# A  Denominator evaluation: details

Below we give a detailed derivation of Eq.(66). The major guideline will be again analysis of pole positions and setting some of the propagators on mass shell by taking appropriate residues.

We first start with the case of strictly forward scattering. (Though it corresponds, of course, to forward elastic $\gamma^* \to \gamma^*$, not $\gamma^* \to V$ scattering, it will not have any effect on the expressions we derive here.) So, the integral to be calculated (see Fig.8) is

$$\int dy\, dz\, d\alpha\, d\beta\ \frac{1}{[(k-\kappa)^2 - m^2 + i\epsilon][k^2 - m^2 + i\epsilon][(k-q)^2 - m^2 + i\epsilon][(k-q-\kappa)^2 - m^2 + i\epsilon]}$$

$$\frac{1}{[\kappa^2 - \mu^2 + i\epsilon]^2[(p-\kappa)^2 - m_p^2 + i\epsilon]} \tag{118}$$

With Sudakov's decomposition (47), one can rewrite all 7 propagators as:

$$
\begin{aligned}
\langle 1\rangle \quad & (k-\kappa)^2 - m^2 + i\epsilon = (-y-\alpha)(z+\beta)s - ((\vec{k}-\vec{\kappa})^2 + m^2 - i\epsilon)\,, \\
\langle 2\rangle \quad & k^2 - m^2 + i\epsilon = -szy - (\vec{k}^2 + m^2 - i\epsilon)\,, \\
\langle 3\rangle \quad & (k-q)^2 - m^2 + i\epsilon = (-y+x)(z-1)s - (\vec{k}^2 + m^2 - i\epsilon)\,, \\
\langle 4\rangle \quad & (k-q-\kappa)^2 - m^2 + i\epsilon = (-y+x-\alpha)(z-1+\beta)s - ((\vec{k}-\vec{\kappa})^2 + m^2 - i\epsilon)\,, \\
\langle 5,6\rangle \quad & \kappa^2 - \mu^2 + i\epsilon = -\alpha\beta s - (\vec{\kappa}^2 + \mu^2 - i\epsilon)\,, \\
\langle 7\rangle \quad & (p-\kappa)^2 - m_p^2 + i\epsilon = (1-\alpha)\beta s - (\vec{\kappa}^2 + m_p^2 - i\epsilon)\,.
\end{aligned}
\tag{119}
$$

After an accurate analysis of position of all poles on complex $\alpha, \beta, y$ planes, one finds that the only non-zero contribution survives if one uses line $\langle 4\rangle$ to extract $\alpha$, line $\langle 2\rangle$ to extract $y$ and line $\langle 7\rangle$ to extract $\beta$:

$$\alpha = -y + x + \frac{(\vec{k}-\vec{\kappa})^2 + m^2}{(1-z)s}; \quad y = -\frac{\vec{k}^2 + m^2}{zs}; \quad \beta = \frac{\vec{\kappa}^2 + \mu^2}{s}\,. \tag{120}$$

Note that resultant $\alpha, \beta, y \ll 1$. The remaining $z$-integration goes from 0 to 1. Therefore, integral (118) turns into

$$\left(-\frac{2\pi i}{s}\right)^3 \cdot \int_0^1 \frac{dz}{z} \frac{1}{1-z} \cdot \frac{1}{\langle 5\rangle\langle 6\rangle\langle 1\rangle\langle 3\rangle}\,, \tag{121}$$

where the numbers in brackets denote the corresponding propagators. With aid of (120), these propagators become:

$$
\begin{aligned}
\langle 5,6\rangle \quad & -\alpha\beta s - (\vec{\kappa}^2 + \mu^2) \approx -(\vec{\kappa}^2 + \mu^2) \\
\langle 3\rangle \quad & y(1-z)s - xs(1-z) - (\vec{k}^2 + m^2) = -\frac{1}{z}[\vec{k}^2 + m^2 + z(1-z)Q^2] \\
\langle 1\rangle \quad & -(y+\alpha-x)zs - [(\vec{k}-\vec{\kappa})^2 + m^2] = -\frac{1}{1-z}[(\vec{k}-\vec{\kappa})^2 + m^2 + z(1-z)Q^2]
\end{aligned}
\tag{122}
$$

Here we used $\alpha \ll 1$. Substituting these expressions into (121), one gets

$$\left(-\frac{2\pi i}{s}\right)^3 \cdot \int_0^1 \frac{dz}{(\vec{\kappa}^2 + \mu^2)^2} \frac{1}{[\vec{k}^2 + m^2 + z(1-z)Q^2][(\vec{k}-\vec{\kappa})^2 + m^2 + z(1-z)Q^2]}\,. \tag{123}$$

Note that we replaced the lower integration limit by zero, knowing that there is no large end-point contribution.

In the above analysis we took momentum transfer $\vec{\Delta} = 0$ for simplicity. Now let us see what non-zero momentum transfer will change (see Fig.(8)).

First of all, now $\vec{\Delta}$ will appear in gluon propagators. However, condition (68) allows us to neglect it within diffraction cone. Then, $\vec{\Delta}$ will enter quark loop propagators. Here the presence of momentum transfer (especially, the longitudinal one) is very important. Indeed, within our notation of momenta, the propagator pair $\langle 1, 4 \rangle$ will yield the same contribution as before

$$\vec{k}_1^2 + m^2 + z(1-z)Q^2 \,,$$

where $\vec{k}_1$ is transverse momentum flowing through the photon vertex. On the other hand, propagators $\langle 2, 3 \rangle$ will give now

$$\vec{k}^2 + m^2 - z(1-z)m_V^2 \,,$$

which together with vertex factor $\Gamma$ gives rise to the vector meson LCWF. Combining everything together, one now has

$$\int dy \, dz \, d\alpha \, d\beta \, \frac{\Gamma}{[\text{all propagators}]}$$
$$= \left( -\frac{2\pi i}{s} \right)^3 \cdot \int \frac{dz}{z(1-z)} \psi(z, \vec{k}^2) \cdot \frac{1}{\vec{k}_1^2 + m^2 + z(1-z)Q^2} \, \frac{1}{(\vec{\kappa}^2 + \mu^2)^2} \qquad (124)$$

# B   Helicity amplitude technique evaluation

Here we give the derivation of expression for traces of the following type

$$Sp\left\{\hat{e}\ (\hat{k}_4 + m)\ \hat{p}'\ (\hat{k}_3 + m)\ \hat{V}^*\ (\hat{k}_2 + m)\ \hat{p}'\ (\hat{k}_1 + m)\right\} \tag{125}$$

in full detail. Though one can calculate this trace covariantly, a particularly convenient way to do so is given by light cone helicity amplitude technique [17]. We emphasize that both ways are absolutely equivalent. In the helicity amplitude approach, we recall that all fermion lines in (125) can be taken on mass shell (see detailed derivation of LCWF normalization in Sect.2.5) and decomposed into a sum of light cone helicities

$$(\hat{k} + m) \rightarrow \sum_{\lambda = \pm} u_\lambda \bar{u}_\lambda \quad \text{for quark lines};$$

$$(\hat{k} + m) = -[(-\hat{k}) - m] \rightarrow -\sum_{\lambda = \pm} v_\lambda \bar{v}_\lambda \quad \text{for antiquark lines}.$$

Since the specific choice of this decomposition does not affect the final result, we are free to take the most convenient choice of spinors (see [17] for details), namely,

$$u(p, \lambda) = \frac{1}{\sqrt{\sqrt{2}p^+}} \left(\sqrt{2}p^+ + \beta m + \vec{\alpha}\vec{p}\right) \begin{cases} \chi(\uparrow) & \lambda = +1 \\ \chi(\downarrow) & \lambda = -1 \end{cases}$$

$$v(p, \lambda) = \frac{1}{\sqrt{\sqrt{2}p^+}} \left(\sqrt{2}p^+ - \beta m + \vec{\alpha}\vec{p}\right) \begin{cases} \chi(\downarrow) & \lambda = +1 \\ \chi(\uparrow) & \lambda = -1 \end{cases} \tag{126}$$

where

$$\chi(\uparrow) = \frac{1}{\sqrt{2}} \begin{pmatrix} 1 \\ 0 \\ 1 \\ 0 \end{pmatrix} ; \quad \chi(\downarrow) = \frac{1}{\sqrt{2}} \begin{pmatrix} 0 \\ 1 \\ 0 \\ -1 \end{pmatrix}$$

It is a straightforward exercise to show that they obey usual normalization and completeness requirements:

$$\bar{u}(p, \lambda)u(p, \lambda') = -\bar{v}(p, \lambda)v(p, \lambda') = 2m\delta_{\lambda\lambda'} ;$$

$$\sum_\lambda u(p, \lambda)\bar{u}(p, \lambda) = \hat{p} + m ; \quad \sum_\lambda v(p, \lambda)\bar{v}(p, \lambda) = \hat{p} - m . \tag{127}$$

Thus, expression (125) turns into

$$2s^2 \cdot I^{(c)} = (-1)^2 \sum_{\lambda_i} \bar{u}\hat{e}v \cdot \bar{v}\hat{p}'v \cdot \bar{v}\hat{V}^*u \cdot \bar{u}\hat{p}'u \cdot . \tag{128}$$

Though this expression is written for Diagr.7c, one can immediately redo the same transformation for the other diagrams. So, in the following we first list the light cone helicity amplitudes to be used later. Then, we derive the amplitudes for photon and vector meson vertices $\bar{u}\hat{e}v$ and $\bar{v}\hat{V}^*u$ respectively with appropriate polarization vectors. Finally, we give a simple rule of how to include 2 gluon legs attachments (i.e. $\bar{u}\hat{p}'u$ and $\bar{v}\hat{p}'v$) and write the final expressions.

## B.1 List of helicity amplitudes

Here we list various amplitudes of $\bar{u}'_{\lambda_1}(p)...u_{\lambda_2}(q)$ type various gamma matrix structures inserted between light cone spinors. This notation should not be confused with our previous usage of $p$ and $q$; here and only here these momenta are assigned to the fermion lines as shown at Fig.15.
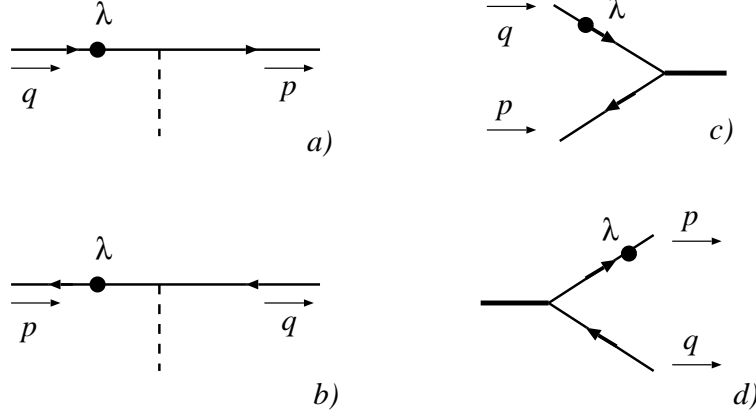
For a derivation of these amplitudes see [17].



Figure 15: Four types of transitions for which the light cone helicity amplitudes are given below. The dot with label $\lambda$ indicates the spinor, whose helicity is used as $\lambda$ in the table of amplitudes.

Notation:
as usual, each vector $\vec{a}$ should be understood as $\vec{a}_\perp$,
momenta $p$ and $q$ are constituent momenta shown at relevant figures;
For $\lambda = \pm 1$ we define

$$a(\lambda) = -\lambda a_x - ia_y . \tag{129}$$

'Cross product' is defined as

$$[\vec{a}\vec{b}] = a_x b_y - b_x a_y . \tag{130}$$

(This is not a true cross product of two vectors, this is just a handy notation.) Moreover **every** matrix element should be multiplied by common factor $\sqrt{p_+ q_+}$.

### B.1.1 Straight line elements

Fig.15a:

|  | $\bar{u}_\lambda(p)...u_\lambda(q)$ | $\bar{u}_{-\lambda}(p)...u_\lambda(q)$ |
|---|---|---|
| $\gamma^+$ | $2$ | $0$ |
| $\gamma^-$ | $\frac{1}{p_+ q_+}(m^2 + \vec{p}\vec{q} + i\lambda[\vec{p}\vec{q}])$ | $\frac{m}{p_+ q_+}(p(\lambda) - q(\lambda))$ |
| $\vec{a}\cdot\vec{\gamma}$ | $\frac{\vec{a}\vec{p}}{p_+} + \frac{\vec{a}\vec{q}}{q_+} - i\lambda\left(\frac{[\vec{a}\vec{p}]}{p_+} - \frac{[\vec{a}\vec{q}]}{q_+}\right)$ | $-ma(\lambda)\left(\frac{1}{p_+} - \frac{1}{q_+}\right)$ |

$$\tag{131}$$

Fig.15b

$$\bar{v}_\lambda(p)...v_\lambda(q) \qquad\qquad \bar{v}_\lambda(p)...v_{-\lambda}(q)$$

$$
\begin{array}{ccc}
\gamma^+ & 2 & 0 \\[4pt]
\gamma^- & \dfrac{1}{p_+ q_+}\left(m^2 + \vec{p}\vec{q} - i\lambda[\vec{p}\vec{q}]\right) & -\dfrac{m}{p_+ q_+}\left(p(\lambda) - q(\lambda)\right) \\[10pt]
\vec{a}\cdot\vec{\gamma} & \dfrac{\vec{a}\vec{p}}{p_+} + \dfrac{\vec{a}\vec{q}}{q_+} + i\lambda\left(\dfrac{[\vec{a}\vec{p}]}{p_+} - \dfrac{[\vec{a}\vec{q}]}{q_+}\right) & ma(\lambda)\left(\dfrac{1}{p_+} - \dfrac{1}{q_+}\right)
\end{array}
\tag{132}
$$

## B.1.2  Vertex lines

Fig.15c

$$\bar{v}_\lambda(p)...u_\lambda(q) \qquad \bar{v}_{-\lambda}(p)...u_\lambda(q)$$

$$
\begin{array}{ccc}
\gamma^+ & 0 & 2 \\[4pt]
\gamma^- & \dfrac{m}{p_+ q_+}\left(p(\lambda) + q(\lambda)\right) & \dfrac{1}{p_+ q_+}\left(-m^2 + \vec{p}\vec{q} + i\lambda[\vec{p}\vec{q}]\right) \\[10pt]
\vec{a}\cdot\vec{\gamma} & ma(\lambda)\left(\dfrac{1}{p_+} + \dfrac{1}{q_+}\right) & \dfrac{\vec{a}\vec{p}}{p_+} + \dfrac{\vec{a}\vec{q}}{q_+} - i\lambda\left(\dfrac{[\vec{a}\vec{p}]}{p_+} - \dfrac{[\vec{a}\vec{q}]}{q_+}\right)
\end{array}
$$

Fig.15d

$$\bar{u}_\lambda(p)...v_\lambda(q) \qquad\qquad \bar{u}_\lambda(p)...v_{-\lambda}(q)$$

$$
\begin{array}{ccc}
\gamma^+ & 0 & 2 \\[4pt]
\gamma^- & -\dfrac{m}{p_+ q_+}\left(p(-\lambda) + q(-\lambda)\right) & \dfrac{1}{p_+ q_+}\left(-m^2 + \vec{p}\vec{q} + i\lambda[\vec{p}\vec{q}]\right) \\[10pt]
\vec{a}\cdot\vec{\gamma} & -ma(-\lambda)\left(\dfrac{1}{p_+} + \dfrac{1}{q_+}\right) & \dfrac{\vec{a}\vec{p}}{p_+} + \dfrac{\vec{a}\vec{q}}{q_+} - i\lambda\left(\dfrac{[\vec{a}\vec{p}]}{p_+} - \dfrac{[\vec{a}\vec{q}]}{q_+}\right)
\end{array}
$$

## B.2  Photon vertex amplitudes

Notation is given in Fig.8. We start with transverse photon.

$$\bar{u}'\hat{e}_T v = \bar{u}'(-\vec{\gamma}\vec{e})v\,.$$

Equal $q\bar{q}$ helicities give

$$-\frac{\sqrt{z(1-z)}q_+}{z(1-z)q_+}\cdot(-m)e(-\lambda) = \frac{1}{\sqrt{z(1-z)}}me(-\lambda) \tag{133}$$

Opposite $q\bar{q}$ helicities give

$$-\frac{\sqrt{z(1-z)}q_+}{z(1-z)q_+}\cdot\left[(\vec{e}\vec{k_1})(1-z) - (\vec{e}\vec{k_1})z - i\lambda\left([\vec{e}\vec{k_1}](1-z) + [\vec{e}\vec{k_1}]z\right)\right]$$

$$= -\frac{1}{\sqrt{z(1-z)}}\left[(\vec{e}\vec{k_1})(1-2z) - i\lambda[\vec{e}\vec{k_1}]\right] \tag{134}$$

In the case of scalar photon

$$\bar{u}'\hat{e}_0 v = \bar{u}'\frac{1}{Q}(q_+\gamma_- + xp_-\gamma_+)v$$

the same helicities give exactly zero while opposite helicities result in

$$\frac{\sqrt{z(1-z)}q_+}{z(1-z)q_+} \cdot \frac{1}{Q} \cdot \left[\frac{q_+}{q_+}(-m^2 - \vec{k}_1^2) + x2z(1-z)p_-q_+\right]$$
$$= -\frac{1}{\sqrt{z(1-z)}}\frac{1}{Q}\left[m^2 + \vec{k}_1^2 - z(1-z)Q^2\right] \tag{135}$$

## B.3   Vector meson vertex amplitudes

This case is more tricky due to the nonzero vector meson transverse momentum $\vec{\Delta}$. We start with the transverse vector meson polarization:

$$\hat{V}_T^* = -\vec{\gamma}\vec{V}^* + \frac{2(\vec{V}^*\vec{\Delta})}{s}p_-\gamma_+ \, .$$

The same $q\bar{q}$ helicities give again

$$-\frac{\sqrt{z(1-z)}q_+}{z(1-z)q_+} \cdot mV^*(\lambda) = -\frac{1}{\sqrt{z(1-z)}}mV^*(\lambda) \tag{136}$$

while opposite helicities give

$$\frac{\sqrt{z(1-z)}q_+}{z(1-z)q_+}\left\{-[(\vec{V}^*\vec{k}_3)z + (\vec{V}^*\vec{k}_2)(1-z) - i\lambda\left([\vec{V}^*\vec{k}_3]z - [\vec{V}^*\vec{k}_2](1-z))\right)]\right.$$
$$\left.+\frac{2(\vec{V}^*\vec{\Delta})}{s}p_-2z(1-z)q_+\right\}$$
$$= -\frac{1}{\sqrt{z(1-z)}}\left\{(\vec{V}^*\vec{k})(1-2z) + i\lambda[V\vec{k}]\right\} \tag{137}$$

Here we used definitions and properties (see also Fig.8):

$$\vec{k}_2 = \vec{k} + z\vec{\Delta}; \quad \vec{k}_3 = -\vec{k} + (1-z)\vec{\Delta} \tag{138}$$
$$\Rightarrow \quad (1-z)\vec{k}_2 - z\vec{k}_3 = \vec{k}; \quad (1-z)\vec{k}_2 + z\vec{k}_3 = (1-2z)\vec{k} + 2z(1-z)\vec{\Delta};$$
$$(\vec{k}_2\vec{k}_3) = -\vec{k}^2 + (1-2z)(\vec{k}\vec{\Delta}) + z(1-z)\vec{\Delta}^2$$
$$M^2 + \vec{\Delta}^2 = \frac{\vec{k}_2^2 + m^2}{z} + \frac{\vec{k}_3^2 + m^2}{(1-z)} = \frac{\vec{k}^2 + m^2}{z(1-z)} + \vec{\Delta}^2 \, .$$

For the longitudinal vector mesons one has for equal quark-antiquark helicities

$$\frac{\sqrt{z(1-z)}q_+}{z(1-z)q_+}\frac{1}{M} \cdot \left[-m\vec{\Delta}(\lambda) + m\frac{q_+}{q_+}[k_2(\lambda) + k_3(\lambda)]\right] = 0 \tag{139}$$

and for opposite helicities

$$\frac{\sqrt{z(1-z)}q_+}{z(1-z)q_+}\frac{1}{M}\left\{-[(\vec{\Delta}\vec{k}_3)z + (\vec{\Delta}\vec{k}_2)(1-z) + i\lambda[\vec{\Delta}\vec{k}]] + \frac{q_+}{q_+}[-m^2 + (\vec{k}_2\vec{k}_3) + i\lambda[\vec{k}_3\vec{k}_2]]\right.$$
$$\left. + \frac{\vec{\Delta}^2 - M^2}{s}p_-2z(1-z)q_+\right\}$$
$$= -\frac{1}{\sqrt{z(1-z)}}2z(1-z)M \tag{140}$$

## B.4   Final trace calculation

Once we have the expressions for vertex amplitudes, the rest is done quickly. We first note that each gluon vertex attached to the lower or upper line gives factor

$$2zq_+ \cdot p_- = sz; \quad 2(1-z)q_+ \cdot p_- = s(1-z) \tag{141}$$

correspondingly.

So. let's start with $T \to T$ amplitude and calculate it for Diagr.(c) at Fig.7.

Equal $q\bar{q}$ helicities give

$$s(1-z) \cdot sz \cdot \frac{-1}{\sqrt{z(1-z)}}mV^*(\lambda)\frac{1}{\sqrt{z(1-z)}}me(-\lambda) = -s^2m^2e(-\lambda)V^*(\lambda) \tag{142}$$

Summing over $\lambda$ gives

$$2s^2m^2(\vec{e}\vec{V}^*). \tag{143}$$

The opposite helicities yield

$$s^2\left[(\vec{V}^*\vec{k})(1-2z) + i\lambda[\vec{V}^*\vec{k}]\right]\left[(\vec{e}\vec{k}_1)(1-2z) - i\lambda[\vec{e}\vec{k}_1]\right] \tag{144}$$

Summing over helicities and making use of identity

$$[\vec{a}\vec{b}][\vec{c}\vec{d}] = (\vec{a}\vec{c})(\vec{b}\vec{d}) - (\vec{a}\vec{d})(\vec{b}\vec{c}) \tag{145}$$

one obtains

$$2s^2\left[(\vec{V}^*\vec{k})(\vec{e}\vec{k}_1)(1-2z)^2 + (\vec{e}\vec{V}^*)(\vec{k}\vec{k}_1) - (\vec{e}\vec{k})(\vec{V}^*\vec{k}_1)\right]. \tag{146}$$

Since we factored out $2s^2$ when deriving (64), we finally get

$$I^{(c)}_{T\to T} = -\left[(\vec{e}\vec{V}^*)(m^2 + \vec{k}\vec{k}_1) + (\vec{V}^*\vec{k})(\vec{e}\vec{k}_1)(1-2z)^2 - (\vec{e}\vec{k})(\vec{V}^*\vec{k}_1)\right]. \tag{147}$$

We included factor $(-1)$ since in this diagram we have one antiquark propagator.

An important observation here is that all other integrands, namely $I^{(a)} \cdot (1-z)/z$, $I^{(c)}, I^{(d)} \cdot z/(1-z)$ give absolutely the same result (with their own definitions of $\vec{k}_1$ of course). The only thing one should not forget is that diagrams (a,d) enter with sign '$-$' while diagrams (b,c) enter with sign '$+$':

$$-\frac{1-z}{z}I^{(a)} = I^{(b)} = I^{(c)} = -\frac{z}{1-z}I^{(d)}.$$

For $L \to L$ amplitude one has immediately

$$I_{L \to L}^{(c)} = -\frac{1}{Q}[m^2 + \vec{k}_1^2 - z(1-z)Q^2] \cdot \frac{1}{M}2z(1-z)M^2 \tag{148}$$

In fact, using simple relation

$$\frac{m^2 + \vec{k}_1^2 - z(1-z)Q^2}{m^2 + \vec{k}_1^2 + z(1-z)Q^2} = 1 + \frac{-2z(1-z)Q^2}{m^2 + \vec{k}_1^2 + z(1-z)Q^2} \tag{149}$$

and noting that all unity terms will eventually cancel out in (72), one can rewrite (148) as

$$I_{L \to L}^{(c)} = -4QMz^2(1-z)^2 \,. \tag{150}$$

For $T \to L$ amplitude one has

$$I_{T \to L}^{(c)} = 2z(1-z)M(\vec{e}\vec{k}_1)(1-2z) \tag{151}$$

and for $L \to T$ amplitude one has

$$I_{L \to T}^{(c)} = \frac{1}{Q}[m^2 + \vec{k}_1^2 - z(1-z)Q^2](1-2z)(\vec{V}^*\vec{k}) \,. \tag{152}$$

The same transformation as in $L \to L$ amplitude, leads to

$$I_{L \to T}^{(c)} = -2z(1-z)Q^2(1-2z)(\vec{V}^*\vec{k}) \,. \tag{153}$$

Note that in the last three amplitudes only opposite $q\bar{q}$ helicities contributed.

# C   Averaging over $\Omega_{\mathbf{p}}$ for $D$ wave states

Before doing this, let's have a table of useful relations:

$$\langle \vec{k}^2 \rangle = \frac{2}{3}\mathbf{p}^2 \quad \langle p_z^2 \rangle = \frac{1}{3}\mathbf{p}^2$$

$$\langle \vec{k}^2 \vec{k}^2 \rangle = \frac{8}{15}\mathbf{p}^4 \quad \langle \vec{k}^2 p_z^2 \rangle = \frac{2}{15}\mathbf{p}^4 \quad \langle p_z^2 p_z^2 \rangle = \frac{3}{15}\mathbf{p}^4 \tag{154}$$

Finally, remember that $p_z^2 = \frac{1}{4}(1-2z)^2 M^2$.

One has to perform the following avegaring

$$\left\langle 4z(1-z) \cdot \frac{1}{\overline{Q}^4} \cdot \left( \vec{k}^2 - \frac{4m}{M}p_z^2 \right) \cdot \left( 1 - \frac{4\vec{k}^2}{\overline{Q}^2} \right) \right\rangle \tag{155}$$

Note that all factors should be carefully examined; all four do contribute to the final answer. Decomposing $\overline{Q}^2$ as

$$\overline{Q}^2 = m^2 + z(1-z)Q^2 = m^2 + \frac{1}{4}Q^2 - \frac{1}{4}(1-2z)^2 Q^2 \equiv \overline{Q}_0^2 - \frac{p_z^2}{M^2}Q^2, \tag{156}$$

one gets

$$\frac{1}{\overline{Q}^4} = \frac{1}{\overline{Q}_0^4}\left( 1 + 2\frac{p_z^2}{M^2}\frac{Q^2}{\overline{Q}_0^2} \right). \tag{157}$$

So, omitting $\overline{Q}_0^{-4}$, one has

$$\left\langle \left( 1 - \frac{4p_z^2}{M^2} \right) \cdot \left( 1 + 2\frac{p_z^2}{M^2}\frac{Q^2}{\overline{Q}_0^2} \right) \cdot \left( \vec{k}^2 - \frac{4m}{M}p_z^2 \right) \cdot \left( 1 - \frac{4\vec{k}^2}{\overline{Q}_0^2} \right) \right\rangle \tag{158}$$

With the aid of (100), one obtains

$$\left\langle \vec{k}^2 - \frac{4m}{M}p_z^2 \right\rangle - \frac{4}{M^2}\left\langle \vec{k}^2 p_z^2 - 2p_z^2 p_z^2 \right\rangle + 2\frac{Q^2}{M^2\overline{Q}_0^2}\left\langle \vec{k}^2 p_z^2 - 2p_z^2 p_z^2 \right\rangle - \frac{4}{\overline{Q}_0^2}\left\langle \vec{k}^2 \vec{k}^2 - 2p_z^2 \vec{k}^2 \right\rangle$$

$$= \left( \frac{2}{3}\mathbf{p}^2 - \frac{4m}{3M}\mathbf{p}^2 \right) - \frac{4}{M^2}\mathbf{p}^4\left( \frac{2}{15} - \frac{6}{15} \right) + 2\frac{Q^2}{M^2\overline{Q}_0^2}\mathbf{p}^4\left( \frac{2}{15} - \frac{6}{15} \right) - \frac{4}{\overline{Q}_0^2}\mathbf{p}^4\left( \frac{8}{15} - \frac{4}{15} \right)$$

$$= \frac{2}{3}\mathbf{p}^2\frac{4\mathbf{p}^2}{M+2m} + \frac{16\mathbf{p}^4}{15M^2} - \frac{8Q^2\mathbf{p}^4}{15M^2\overline{Q}_0^2} - \frac{16\mathbf{p}^4}{15\overline{Q}_0^2} \tag{159}$$

$$= \frac{4\mathbf{p}^4}{3M^2}\left( 1 + \frac{4}{5} - \frac{8}{5}\frac{Q^2}{Q^2+M^2} - \frac{16}{5}\frac{M^2}{Q^2+M^2} \right)$$

$$= \frac{4\mathbf{p}^4}{15M^2}\left( 1 - 8\frac{M^2}{Q^2+M^2} \right)$$

For the helicity conserving $T \to T$ amplitude one has to repeat the same averaging procedure. The expression to be calculated first is

$$\left\langle \left( 1 + 2\frac{p_z^2}{M^2}\frac{Q^2}{\overline{Q}_0^2} \right) \cdot \left[ 2\mathbf{p}^2\left( m^2 + 2\vec{k}^2 - 4\vec{k}^2\frac{m^2}{\overline{Q}^2} \right) - m(M+m)\vec{k}^2\left( 1 - \frac{4\vec{k}^2}{\overline{Q}^2} \right) - 2\vec{k}^2\left( \vec{k}^2 - \frac{4m}{M}p_z^2 \right) \right] \right\rangle$$

$$= 2m^2\mathbf{p}^2 - \frac{2}{3}m(M+m)\mathbf{p}^2 + 2\frac{p_z^2}{M^2}\frac{Q^2}{Q_0^2}\left(\frac{1}{2}M^2\frac{1}{3} - 3M^2\frac{2}{15}\right) + \frac{8}{3}\mathbf{p}^4 - \frac{8}{15}\mathbf{p}^4 + \frac{m^2}{Q_0^2}\mathbf{p}^4\frac{16}{15}$$

$$= -\frac{2}{3}\mathbf{p}^4 - \frac{8}{15}\mathbf{p}^4 + \frac{8}{3}\mathbf{p}^4 + \frac{16}{15}\frac{M^2}{M^2+Q^2}\mathbf{p}^4 + \frac{8}{15}\frac{Q^2}{M^2+Q^2}\mathbf{p}^4$$

$$= 2\mathbf{p}^4\left(1 + \frac{4}{15}\frac{M^2}{M^2+Q^2}\right). \tag{160}$$

# Acknowledgements

# Curriculum Vitae

1. Name - Igor Ivanov

2. Date of birth - 26 October 1976

3. Place of birth - Petropavlovsk-Kamchatsky, Russia

4. Educational and scientific background:

   — graduated from Physics and Mathematics School at Novosibirsk University in June 1993;

   — received Physics Bachelor Diploma of Novosibirsk University in July 1997. My Bachelor Diploma Research was based on ref.[1].

   — 1998–1999: graduate student (Studentenhilfskraft) at Institüt für Kernphysik, Forschungszentrum Jülich, Germany

   — received MSc Diploma in Physics of Novosibirsk University in June 1999.

   — currently PhD student of Novosibirsk University and Doktorand at Institüt für Kernphysik,
   Forschungszentrum Jülich

5. Teaching experience - I have been teaching physics seminars and the elective course 'Olympiad problems in physics' at the Physics and Mathematics School (Novosibirsk) for three years.

6. Publications:

   [1] I.F.Ginzburg, I.P.Ivanov *'Higgs boson search at photon colliders for $M_H = 140 - 190$ GeV', Phys.Lett.* **B408** (1997) 325; **hep-ph/9704220**.

   [2] I.F Ginzburg, I.P.Ivanov, A. Schiller *'Search for Next Generations of Quarks and Leptons at the Tevatron and LHC',* to appear in *Phys. Rev. D*; **hep-ph/9802364**.

   [3] A.T.Banin, I.F.Ginzburg, I.P.Ivanov *'Anomalous interactions in Higgs boson production at $\gamma\gamma$ and $e\gamma$ colliders', Phys. Rev.* **D 59** (1999) 115001; **hep-ph/9806515**.

   [4] I.P.Ivanov, N.N.Nikolaev, *Pis'ma ZhETF (JETP Lett.)* **69** (1999) 268; **hep-ph/9901267**.

   [5] I.P.Ivanov, N.N.Nikolaev, A. Pronyaev, W. Schaefer, *Phys. Lett.,* **B 457** (1999), 218-226 ;**hep-ph/9903228**.

7. Fields of interest: quantum field theory, high energy physics, Standard model and beyond, Higgs boson physics, high energy photon interactions, QCD, diffractive deep-inelastic processes, spin structure functions.